



Total Control

Advanced integrated supervisory and wind turbine control for optimal operation of large Wind Power Plants

Title: Cost model for fatigue degradation and O&M
Deliverable no.: 2.1

*Delivery date: 19.12.2018
Lead beneficiary: SINTEF
Dissemination level: PU*



This project has received funding from the European Union's Horizon 2020 Research and Innovation Programme under grant agreement No. 727680

Author(s) information (alphabetical):		
Name	Organisation	Email
Salvatore D'Arco	SINTEF Energy Research	salvatore.darco@sintef.no
Martin Evans	DNV GL	martin.evans@dnvgl.com
Jørn Foros	SINTEF Energy Research	jorn.foros@sintef.no
Anand Natarajan	DTU	anat@dtu.dk
Thomas Welte	SINTEF Energy Research	thomas.welte@sintef.no

Acknowledgements/Contributions:		
Name	Name	Name
Robert Dibble	DNV GL	

Document information

Version	Date	Description			
1.0	19.12.2018	D2.1.1 Cost model for fatigue degradation and O&M	Prepared by Authors listed above	Reviewed by Anand Natarajan	Approved by Gunner Larsen

Definitions

Contents

List of abbreviations.....	4
1. Executive summary	5
2. Introduction.....	7
3. The Impact of WPP Control.....	9
3.1 Existing Literature.....	9
3.2 Cost dependencies.....	9
4. Basic concepts and models.....	11
4.1 Basic concepts.....	11
4.2 Overview of basic cost models	13
4.3 Investment cost model.....	15
4.4 Corrective maintenance cost models.....	16
4.5 Preventive maintenance cost model.....	20
4.6 Design cost model	22
4.7 Summary and discussion.....	22
5. Relative Models for mechanical components	23
6. Models for electrical components.....	27
6.1 Power converters and power cycling reliability.....	27
6.2 Transformers.....	36
7. Wind farm cost model	50
7.1 Details of the Cost Model Framework.....	50
7.2 Details of Individual Component Models	52
8. Conclusions.....	59
References	60
Appendix A – Literature Review	63
Appendix B – Operating time.....	68
B.1 Degradation-equivalent operating time as degradation measure	69
B.2 Relation between degradation, operating time and calendar time	69
Appendix C – Failure rate model and relation to degradation.....	71
C.1 Relation between lifetime/failure rate and degradation	71
C.2 Extension to cases where control strategy is applied to shorter periods	72
Appendix D – Failure rate and hazard rate	74

LIST OF ABBREVIATIONS

AEP	Annual energy production
BEP	Best efficiency point
CAPEX	Capital expenditures
CDF	Cumulative distribution function
CM	Corrective maintenance
CS	Control strategy
DC	Direct current
DP	Degree of polymerization
FOM	Force of mortality
IGBT	Insulated-gate bipolar transistor
LCOE	Levelized cost of energy
MTBF	Mean time between failures
MTTF	Mean time to failure
O&M	Operation and maintenance
OPEX	Operational expenditures
PDF	Probability distribution function
PM	Preventive maintenance
PV	Present value
ROCOF	Rate of occurrence of failure
SF	Survivor function
WPP	Wind power plant
WT	Wind turbine

1. EXECUTIVE SUMMARY

This deliverable is written in work package WP2 in the TotalControl project and summarizes the results from the following sub-tasks in task 2.1 Cost models:

- 2.1.1 – Statistical analysis of the effect of fatigue loading on O&M (operation and maintenance)
- 2.1.2 – Cost of fatigue degradation and O&M of WT (wind turbine) mechanical components
- 2.1.3 – Cost of fatigue degradation and O&M of WPP (wind power plant) electrical components

The main objective of this deliverable is to enable the quantification of the influence of wind farm control on fatigue degradation of mechanical and electrical components and on the O&M cost. The presented models can be used in further work in the TotalControl project for optimization of control strategies, where WPP power production is balanced with cost of WT and WPP loading.

WT and WPP control influence the costs in different ways. First, it influences the energy production. Secondly, it changes the loads on the wind turbine components, which then influences degradation, fatigue and wear, and finally O&M costs. The report presents and discusses several basic models that can be used to quantify the relation between loads, degradation and O&M costs. Furthermore, cost models for fatigue degradation and O&M of mechanical and electrical components are presented. Finally, selected basic and component models are used together in a wind farm cost model. The wind farm cost model can be used to estimate the influence of turbine control on the LCOE and profit of a wind farm.

Control and wind turbine operation can influence different O&M cost elements. Thus, the report discusses which cost elements could be considered as control-dependent. Basic models that can be used to calculate these cost elements are presented and discussed in this report. The basic cost models are called "Investment cost model", "Corrective maintenance cost model", "Preventive maintenance cost model" and "Design cost model" in this report. The O&M costs that are influenced by control and turbine operation can either be represented by one of these cost elements, or the sum of several of them, depending on the scope of the analysis, and the assumptions made. The report discusses which type of costs the different cost elements represent, how they can be calculated, what the similarities and differences are, and when the cost elements are of relevance to consider in cost calculations. The main focus in this report and in the examples that are presented is on the corrective maintenance cost models, but also the other models are discussed.

A detailed first principles model of mechanical component fatigue degradation is developed, to include rotor thrust and power, wake modelling, fatigue damage and correlation to fatigue failures. The cost is then estimated by computing the change in fatigue damage to the change in material mass to withstand fatigue for the intended duration or increase/reduction in lifetime. Simplified models that translate load reduction to mass reduction or extension of wind turbine life are also presented.

The models for electrical components presented in this report built on degradation models. Models are presented for converters and transformers. The lifetime of these electrical components depends much on the condition of specific sub-components or parts. For the converter, the lifetime is much dominated by the condition and degradation of the switching

devices (i.e. the insulated-gate bipolar transistors (IGBTs)). For the transformer, the lifetime is much dominated by the condition and degradation of the winding insulation material. Both for IGBTs and winding insulation materials, models to estimate degradation and lifetime exist. The models are presented in this report and their use for estimating the influence of control and operation on component lifetime and O&M costs is described and illustrated by examples. The examples presented in the report illustrate that degradation of IGBTs and transformers depend on the operation of the components. This means that the lifetime can be influenced by different operation and control strategies.

The life of IGBTs is much affected by power cycling resulting in thermo-mechanical stresses. Thus, a control strategy that reduces power variation and e.g. keeps the power at a constant level extends the lifetime of converters. The life of the transformer winding insulation is much affected by the temperature level in the transformer and insulation. Thus, a control strategy that reduces the loading and temperature of the transformer extends the lifetime of transformers.

The report presents a cost model for the whole wind farm. Selected basic cost models and component models that are earlier introduced and discussed in the report are implemented in the wind farm model. The model estimates the influence of turbine control on the wind, the energy production, the loads on different components, the O&M costs, and finally the LCOE and profit of a wind farm. To achieve this model, wake effects and their influence on power production are considered. Thus, the model implemented as an MS Excel based tool includes wake turbulence and wake deficits, and it quantifies the impact on fatigue damage and power capture. It then translates these effects into increase/decrease of failure rates of components and the costs.

Selected topics are further detailed and discussed in the appendixes of the report. The results from a literature study can also be found in the appendix of the report.

The results presented in this report show that there is a large potential for O&M cost reduction by using advanced control strategies that reduce the loads and increase the lifetime of the components. Further work must balance these benefits with the effects on energy production and wind farm ancillary services. This means that the models presented in this report can be used in TotalControl to optimize WT and WPP control strategies.

2. INTRODUCTION

The scope of this report is to establish models for fatigue degradation and O&M costs that can be included in optimization of wind farm control. Hence, the model should estimate the cost associated with some control decision. Based on the operating conditions on the wind farm, wind farm controllers can vary yaw, speed and torque set points for different wind turbines in the farm¹. The effect of such set point variation on degradation, remaining life, O&M cost and thereby the OPEX under these conditions can be quantified using the models developed herein. The cost model includes several of the turbine components and include both repairable and non-repairable components.

The intention is for potential control schemes to be optimised in other tasks in TotalControl work package WP2, to minimise cost of energy subject to physical constraints of the components.

In general, a wind turbine will normally be utilized to its full potential, but in some cases it may be relevant to change the control strategy, such as to de-rate selected turbines, even though this means lost production. Such cases may be:

- Providing ancillary services to the grid
- Avoiding failure of components before the planned decommissioning of the wind farm
- Reducing the wake on downwind turbines

The cost model will be useful for assessing possible economic benefits of such cases. The case of avoiding failures is especially relevant when the wind farm is approaching its design life, and for components whose fatigue development can be modelled well through deterministic models.

The application of the models is illustrated with examples for different turbine components. The examples presented in this report use, whenever possible, Lillgrund wind farm as a reference case. Lillgrund farm off the coast of Copenhagen has 48 Siemens 2.3 MW wind turbines.

Available statistics indicate that the following components of a wind turbine have the highest rates of failure, and is therefore most important to include in the aging cost model [1] [2]:

- Pitch
- Generator
- Gearbox
- Tower
- Converter

The report is structured as follows:

¹ In this work the developed models are illustrated only with control decisions that are taken as input in the form of a power set point for each turbine over some time interval. However, the cost models are general and may be used for other set points as well.

Section 3 gives the principle relations between WPP control and costs. Important basic concepts that are used for fatigue and cost modelling are introduced in Section 4. Since wind farm control can influence costs in numerous ways, different basic models that can be applied in cost modelling are also presented and discussed in Section 4. Selected basic concepts and models are later used in the specific models that are presented for mechanical and electrical components, as well as the whole wind farm.

Section 5 presents a simplistic approach for mechanical components for translating load reduction to cost reduction. In Section 6, models are presented that describe the relation between turbine operation and degradation of power converters and transformers. We also illustrate the use of the electrical component degradation models in cost modelling.

In Section 7, the work is extended to the whole wind farm and a model is presented for estimating the influence of turbine control on the LCOE and profit of a wind farm. This includes modelling of wake effects and influence on power production.

The report includes also four appendices that contain the results of a literature review and presents additional details and discussions on selected topics.

3. THE IMPACT OF WPP CONTROL ON COSTS

3.1 EXISTING LITERATURE

The existing literature on cost modelling and fatigue was surveyed to ensure that existing work is fully utilised where possible and that the most significant aspects of costs, fatigue and their relationship were identified so that they could be captured in the model. The full literature review is available in Appendix A.

The main learning outcomes from existing literature are:

- The largest costs are the initial capital costs. Therefore, if the fatigue life can be extended, these costs can be spread across an increased lifespan.
- Component costs can be estimated based on component weight or turbine metrics such as rated power or hub height.
- Levelised Cost of Energy is an ideal holistic metric for wind farm performance.
- For mature technologies, O&M cost can be estimated based on historical performance.
- To compare renewables and conventional electricity production methods, the costs of market based carbon offsets should be included.
- The distance to shore influences both the construction and O&M costs, transport vessel hire and fuel costs, and increased amounts of transfer cables to lay and maintain.
- Due of accessibility, the importance of reliability is greater for offshore than onshore.
- The biggest contributor to the overall failure rate for offshore wind turbines is the pitch and hydraulic systems therefore they must be modelled well.
- Each component can have multiple failure modes, of differing severity.
- Failure rates increase with wind speed.
- There is an inverse relationship between downtime for each failure mode and number of technicians deployed to a failure.
- The offshore wind industry is not yet mature enough to provide accurate data as to how component-specific bathtub failure data are expected to vary.
- Opportunistic maintenance (where unplanned corrective maintenance is combined with preventive maintenance carried out on other components) can reduce mobilisation and transport time and costs of vessels.
- Some preventative maintenance can be scheduled during summer when wind speeds are lower and accessibility is higher.
- Must also consider failure of Balance of Plant (such as inter-array and export cables) as well as turbines.
- For large wind power plants, maintenance can be based offshore
- Discrete event, time-sequential Monte Carlo simulation using constant failure rates appear to be the standard method for O&M models.
- Major replacements needing heavy lift vessels (HLVs) accounts for the majority of O&M costs but only make a moderate impact on availability.

3.2 COST DEPENDENCIES

To aid the development of the cost model, the inter-dependencies between aspects of costs were investigated. Once known, the dependencies can be used to determine the requisite flow

of information within the model as well as highlight the aspects that will be influenced by control algorithms or control laws.

FLOWCHART

To visualise the aforementioned dependencies a flow chart was created. The calculations that depend on the control algorithms, directly or indirectly, are highlighted to show the influences that control systems have on the LCOE.

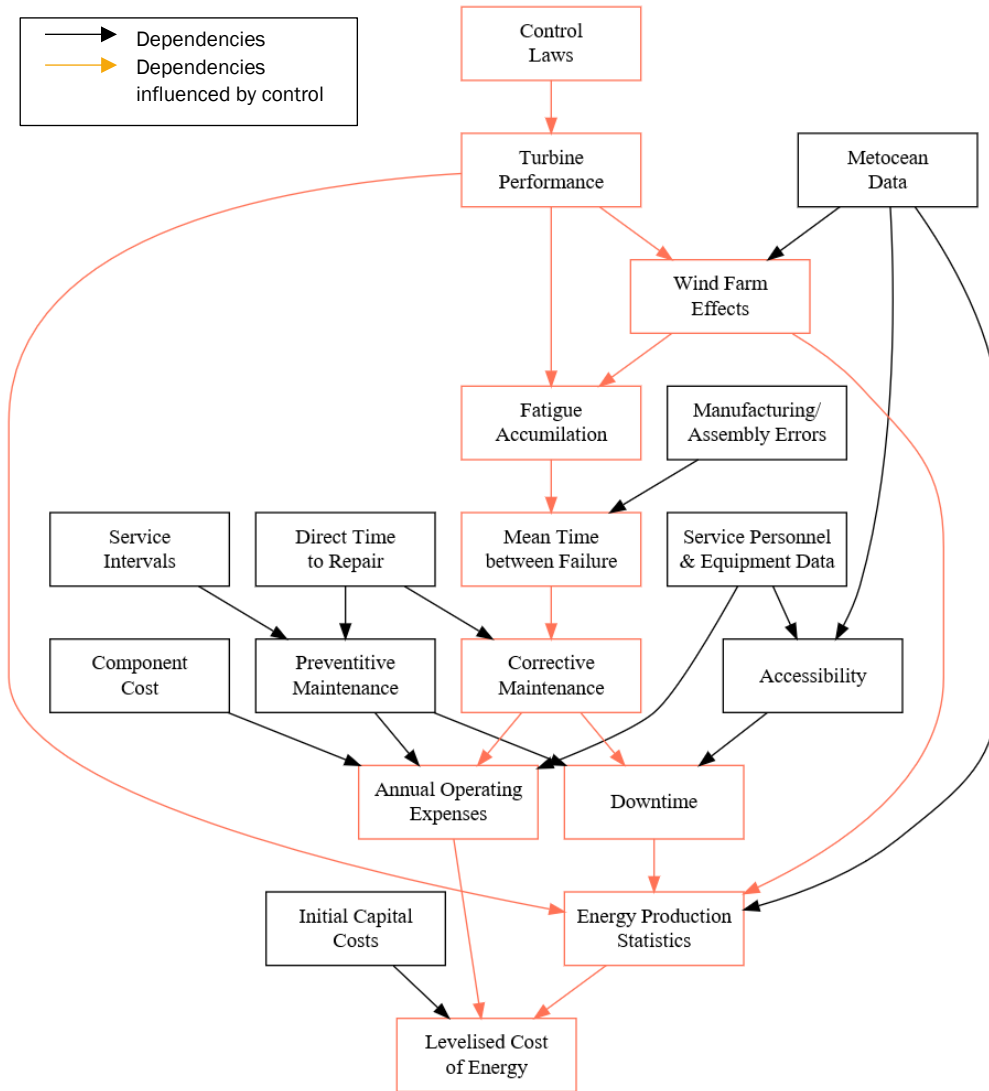


FIGURE 3-1: FLOW CHART FOR RELATIONS BETWEEN WIND TURBINE CONTROL AND LCOE.

CONTROL LAW INFLUENCE

It can be seen from the control influenced dependencies that there are two main influences that the control laws have. First is the impact on the turbine’s energy capture performance, either at the individual turbine level (such as derating) or at the farm level (such as electrical and wake losses). Secondly, is the ability to reduce the wear of components which benefits the corrective maintenance costs and reduces downtime.

4. BASIC CONCEPTS AND MODELS

Several basic cost models that can be used to represent and estimate the influence of control and turbine operation on costs are presented in this section. Furthermore, we briefly introduce and discuss some basic concepts of relevance for degradation and cost modelling.

The following notation is used in this section:

A	Cross section	r	Interest rate
α	Load reduction ratio	SF	Survivor function
C	Cost	σ	Standard deviation of lifetime
C_1	Investment cost	t_{failure}	Failure time
ΔC	Change in cost (increase/decrease)	t_S	Time component has survived
CDF	Cumulative distribution function	t_{WF}	Wind farm lifetime
ε	Failure rate adjustment factor	Δt	Time interval
λ	Failure rate	Δt_{PM}	Extension of time to next preventive maintenance task
L	Exponent	W	Accumulated degradation
$MTBF$	Mean time between failure	ω	Relative degradation
μ	Mean value of lifetime	x	Accumulated degradation or lifetime
PDF	Probability density function	Δx	Fraction of investment cost consumed and written off
ΔPr	Change in failure probability		
PV	Present value		

4.1 BASIC CONCEPTS

CONTROL STRATEGY AND REFERENCE CONTROL STRATEGY

An operational strategy that consists of a set of rules for controlling the wind turbines in a wind farm is denoted *control strategy*. To be able to quantify cost savings or the additional costs of a new control strategy, we must define a baseline or reference control strategy. As a baseline control strategy for a wind turbine and a wind farm, we assume that the wind farm does not have a control system that coordinates control of the individual turbines. That is, the baseline conditions are based on normal operation without any derating of power.

We assume that the lifetime and mean time between failures (MTBF) for a baseline control strategy can be estimated by means of available failure statistics or with a degradation or failure model. The reference MTBF and failure rate are denoted $MTBF_{\text{baseline}}$ and $\lambda_{\text{baseline}}$. The MTBF and failure rate for a new control strategy is denoted $MTBF_{CS}$ and λ_{CS} , respectively.

DEGRADATION MODEL

To be able to quantify the influence of turbine operation and degradation on lifetime, one often uses a degradation model that describes degradation (or wear, fatigue, ageing, etc) over time [3]. In the descriptions of the cost models in section 4, we do not explicitly distinguish between

different degradation mechanisms/failure mechanisms that result in failure of a component. We denote the degradation measure W in the following, where W may be, for example, the accumulated stress, the crack length for a structural component or the degree of polymerization for a transformer. ΔW is the accumulated degradation over a time period Δt .

When degradation reaches W_{failure} , i.e. when the remaining resistance against stress is 0, the component fails. The proportion $\omega = \frac{W}{W_{\text{failure}}}$ is called *relative degradation*. The proportion of relative degradation in a time interval Δt is $\Delta\omega$.

RELATION BETWEEN DEGRADATION AND TIME

One of the basic assumptions in this report is that control changes the loads and degradation. Reduced degradation results in longer lifetime and fewer failures, and lower O&M costs. Depending on the type of failure mechanism, the relation between degradation and time can be linear or non-linear [3], as shown in Figure 4-1. The two examples in the figure illustrate that the relative consumed lifetime ($\Delta t/t_{\text{failure}}$) given the same relative degradation $\Delta\omega$ is different for linear and non-linear² failure mechanisms.

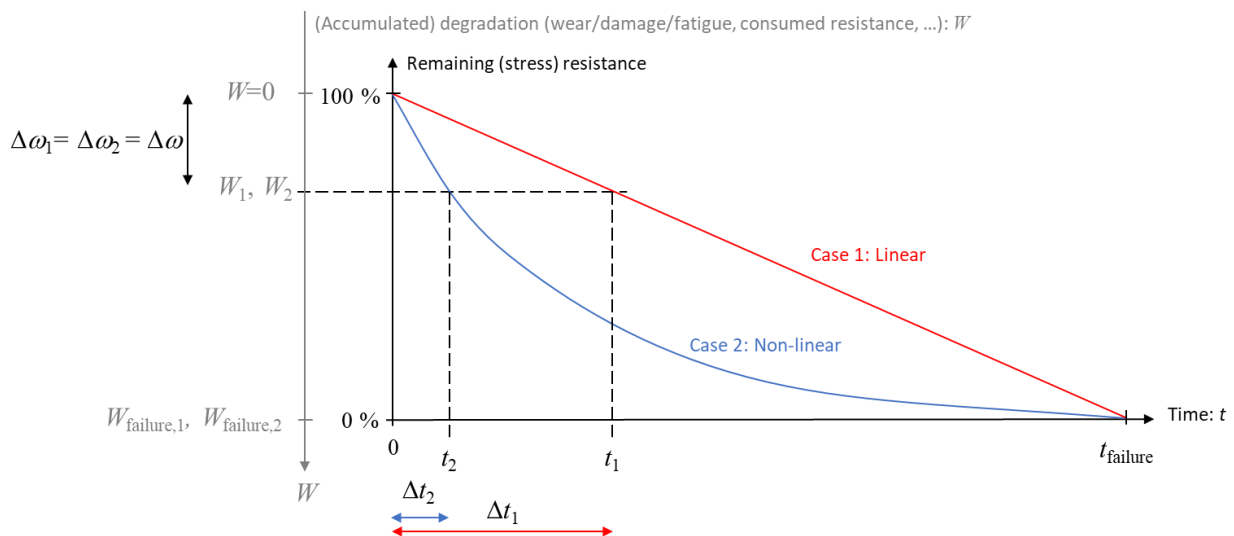


FIGURE 4-1: RELATION BETWEEN MEASURE OF DEGRADATION (W) AND TIME (T) FOR DIFFERENT TYPES OF FAILURE MECHANISMS (LINEAR AND NON-LINEAR).

Time can be measured either in *operating time* or *calendar time*, depending on whether degradation is ongoing only in periods where the turbine or component is in operation.

OPERATING TIME AND CALENDAR TIME

In some cost and degradation models, it is important to distinguish between *operating time* (or *in-service time*) and *calendar time*. As for many technical components, a wind turbine is not operated continuously, since the wind conditions and other factors such as power demand and maintenance require that it is out of operation in some periods. Many turbine components

² For example, as for the degradation model used for the transformer (see section 6.2) where the relation between time t and degradation W , given in degree of polymerisation (DP) in the transformer case, is as illustrated for Case 2.

degrade only or mainly during operation of the wind turbine. In this case, degradation should be related to operating time, instead of calendar time.

We don't apply the concept for operating time in the examples presented in this report. One of the reasons for this is that the models, and the components the models are applied to, do not require to distinguish between calendar time and operating time. However, the difference between calendar time and operating time can be relevant for other applications. A fuller discussion is given in Appendix B.

DISCOUNTING AND INFLATION RATE

The models presented in this report can be extended by discounting future cost with an investment rate. Furthermore, an inflation rate could be used to take into account the increase of future costs. Apart from the model presented in Section 4.5 where discounting is the basic principle of the model, the use of investment and inflation rates is not further discussed and applied in this report. Depending on the future application of the models presented in this report, the use of discounting and inflation should be evaluated.

4.2 OVERVIEW OF BASIC COST MODELS

There are different ways to represent the relation between wind turbine operation and O&M costs and calculate operational costs as a function of turbine operation. Several basic models that can be used for this purpose are presented.

A modified version of Figure 3-1 is shown in Figure 4-2. Four cost elements are highlighted with blue boxes and basic cost models are presented for these cost elements. Table 4-1 briefly describes the models and some assumptions. In general, we assume that the consequences of a changed control strategy are load changes and decreased (or increased) degradation, wear and fatigue. This may influence costs as described in Table 4-1.

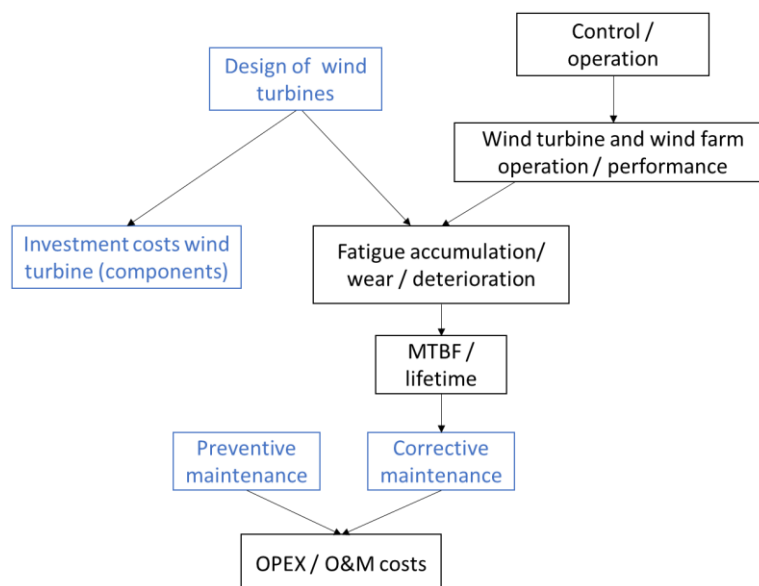


FIGURE 4-2: RELATION BETWEEN CONTROL AND O&M COSTS AND COST ELEMENTS THAT CAN BE CONSIDERED AS O&M COSTS INFLUENCED BY CONTROL (BLUE BOXES) .

TABLE 4-1: BASIC COST MODELS.

Cost model	Description and assumptions
Investment cost model	Operation with a given control strategy consumes a part of the design lifetime of a component. The component represents an investment that has a specific cost (price). The part of the investment cost that corresponds to the design lifetime that is consumed during operation represents the O&M cost, i.e. the investment cost is written off proportional to the part of the lifetime or load that is used by different operational strategies.
Corrective maintenance cost model	As a result of changed loads, the lifetime of components may be increased or decreased. This means that the changed control strategy may extend/reduce lifetime, failure rate and probability of failure. Changes in corrective maintenance costs are the consequence.
Preventive maintenance cost model	A changed preventive maintenance strategy is one possibility to respond to consequences of changed control strategies, e.g. one may reduce the frequency of preventive maintenance actions when control reduces loads.
Design cost model	Changed control strategies that result in reduced loads allow for use of cheaper designs, e.g. by using less material.

Other cost elements that are of importance are increased power production due to less failures and corrective maintenance and due to increased lifetime of the wind farm (i.e. when reduced loads during the design lifetime of 20 years allow for lifetime extension beyond 20 years). When corrective maintenance costs include costs of lost power production, the production losses are considered as part of the corrective maintenance costs. However, the increased power production due to less failures and corrective maintenance can also be modelled explicitly as shown for the wind farm model in Section 7 where the availability and the power production is modelled separately from the corrective maintenance costs. Increased wind farm lifetime can be converted to an increase in power production. However, the effect of wind farm operation on the possibility for lifetime extension is not included in the models presented in this report.

Note that the basic cost models sometimes represent hypothetical situations that would not happen in reality. In a real situation, for example, it is often not possible to replace a component with a new design. Thus, the changes of design costs represent a hypothetical cost change in most cases. Nevertheless, it can be easier in some cases to use such a model to estimate a cost instead of calculating the effects of control on preventive and corrective maintenance costs. Additionally, such models could be used before turbines are selected for a wind farm, to help with that decision or to use wind farm control to help with the business case.

To simplify the cost modelling problem, one may also assume that some of the costs are kept constant, i.e. not influenced by control. One could for example assume that the corrective maintenance cost (including reduced production due to downtime and excluding the option of lifetime extension) represent the total O&M cost if the design of the turbines and the

preventive maintenance strategy are not changed. Another assumption could be that a change in preventive maintenance strategy keeps the number of failures constant. Thus, the changed preventive maintenance costs represent the operational costs (given that the design cannot be changed, and the option of lifetime extension is excluded).

The investment cost model and the design cost model are closely related to each other, because for a given design, a component has a given investment cost. The basic difference between these two cost models is that for the design cost model, we assume that load reduction due to control makes it (hypothetically) possible to use components with cheaper designs (i.e. the investment cost is variable), whereas for the investment cost model, we assume that design and investment costs are fixed and different control strategies influences degradation, which we represent by parts of the investment costs being consumed, or spent.

4.3 INVESTMENT COST MODEL

Control actions and changed control strategy result in changes to wear/fatigue. Wind turbine operation under a given control strategy consumes a part of the lifetime, Δx of a component. That represents an investment that has the investment cost C_I . Then, the cost for operation with a given control strategy can be represented by the fraction of the investment cost that is consumed by a given operational strategy, i.e.:

$$C_{CS} = \Delta x \cdot C_I \quad (1)$$

If Δx is the additional part of the lifetime that is consumed by a new control strategy compared to a baseline strategy, C_{CS} is the additional cost or saved cost for the new control strategy.

The model represents writing off the investment costs relative to the accumulated wear or consumed lifetime within a given time interval. The model has been used in the TOPPFARM wind farm design tool and is described in [4] and [5] where Δx is estimated as a ratio between accumulated equivalent moments (stress) over the considered time interval and the accumulated equivalent moments the component is designed for.

The model has also been used for estimating operational costs of components in hydropower plants, see e.g. Bjørkvoll and Bakken [6], to model the influence of start-up and shut-down of hydropower turbines on the lifetime and costs.

The investment cost model requires the following input:

- Estimate of the relation between turbine control and the accumulated stress or consumed lifetime x .
- Estimate of an investment cost C_I .

DISCUSSION

This model has the drawback that when the initial lifetime is very long, for example when the lifetime of a component is much longer than the wind farm lifetime, the consumption of some lifetime does in practice not result in any costs, since the component is over-designed. Thus, the use of other cost models, for example probabilistic models, that take into account such aspects, may be the better choice.

This model could also be considered as corrective maintenance or a preventive maintenance model, since the investment cost could correspond to the cost for replacing a failed component or preventively replace a component with a new component. The use of the model in such a

setting is described in [5], where also an extension of the model to structural components with probabilistic fatigue criteria is outlined. The relation between the investment cost model and the corrective maintenance model is also discussed in Section 4.4.

CALCULATION OF Δx

Different measures may be used to define Δx . Since we apply a financial model where Δx is multiplied by the investment cost C , and since financial considerations such as discounting are based on time, the most obvious alternative (A1) is to define Δx as the ratio between the consumed lifetime Δt and the total expected lifetime (time to failure or design lifetime) t_{failure} for a baseline load and control case. Another alternative (A2) is to define Δx as relative degradation $\Delta \omega$ (as introduced in section 4.1), i.e. the ratio between accumulated degradation ΔW and the total tolerated degradation W_{failure} .

When the relation between degradation and lifetime is linear, both alternatives (A1, A2) result in the same Δx . However, when the relation between the degradation and lifetime is non-linear, the alternatives result in different Δx ; see Table 4-2, where the calculation alternatives shown in the shaded table cells result in the same Δx . This means that one should consider the underlying degradation process and its relation to time when calculating Δx . The alternatives that are presented in the table are illustrated in Figure 4-1.

TABLE 4-2: DIFFERENT ALTERNATIVES TO CALCULATE Δx AND HOW IT WILL INFLUENCE THE RESULTS FOR DIFFERENT TYPES OF DEGRADATION. GREY CELLS ARE EQUAL DEFINITIONS.

Type of degradation	Alternative A1 (time t)	Alternative A2 (degradation W)
Case C1: Linear	$\Delta x_{C1}^{A1} = \frac{t_1}{t_{\text{failure}}} = \Delta x_{C1}^{A2} = \Delta x_{C2}^{A2}$	$\Delta x_{C1}^{A2} = \frac{W_1}{W_{\text{failure},1}} = \Delta x_{C1}^{A1} = \Delta x_{C2}^{A2}$
Case C2: Non-linear	$\Delta x_{C2}^{A1} = \frac{t_2}{t_{\text{failure}}}$	$\Delta x_{C2}^{A2} = \frac{w_2}{w_{\text{failure},2}} = \Delta x_{C1}^{A2} = \Delta x_{C1}^{A1}$

4.4 CORRECTIVE MAINTENANCE COST MODELS

A changed control strategy may result in changed decreased wear/fatigue, extended lifetime and reduced failure rate and probability of failure. Changes in corrective maintenance costs are the consequence.

Below, two cost models are described that represent corrective maintenance costs, the failure rate model and the lifetime distribution model.

FAILURE RATE MODEL

Assuming that the lifetime is random and thus failure and corrective maintenance occur randomly, we can model relation between failure rate and the costs as described below:

The failure rate λ is the inverse of the mean time between failures (MTBF):

$$\lambda = \frac{1}{MTBF} \quad (2)$$

The average cost for corrective maintenance (CM) is denoted C_{CM} . The mean corrective maintenance cost for a time interval Δt is:

$$C_{CM}(\Delta t) = \lambda \cdot \Delta t \cdot C_{CM} \quad (3)$$

If a new control strategy (e.g. derating) in the time interval Δt reduces the failure rate from $\lambda_{baseline}$ to λ_{CA} , the cost savings ΔC_{CS} of the control strategy compared to a reference strategy are:

$$\Delta C_{CS} = \Delta C_{CM}(\Delta t) = (\lambda_{baseline} - \lambda_{CS}) \cdot \Delta t \cdot C_{CM} \quad (4)$$

Δt is the time interval where we can utilize the effect of the reduced failure rate. Δt is usually the lifetime of the wind farm.

This cost model results in an estimate of average costs. It requires the following input:

- Estimate of failure rate for the reference strategy
 - Note that this reference failure rate must represent the number of failures that can be influenced by control. If the failure rate is taken from statistics, it might be necessary to exclude the portion of the failure rate that cannot be influenced by control.
- Estimate of failure rate for control strategy
 - The failure rate for the control strategy can be estimated based on adjustments as described in the paragraphs below and in the following sections in this report.
- Estimate of corrective maintenance cost, C_{CM}

RELATION BETWEEN FAILURE RATE MODEL AND INVESTMENT COST MODEL

When using the time model for calculation of Δx , i.e. $\Delta x = \frac{\Delta t}{t_{failure}}$ (see section 4.3), we can show that the investment model is equivalent to the failure rate model, provided that Δt is measured in calendar time and $t_{failure} = MTTF \approx MTBF$ (negligible repair time, etc.), and that the investment cost C_I is the same as the costs for replacing the component after failure:

$$C_{CS} = \Delta x C_I = \frac{\Delta t}{t_{failure}} C_{failure} = \frac{1}{MTBF} \Delta t C_{failure} = \lambda \Delta t C_{failure} \quad (5)$$

ESTIMATION OF FAILURE RATE FOR CONTROL STRATEGY BASED ON BASELINE FAILURE RATE

The effect of wind farm control on the failure rate is discussed in this section. We assume that the failure rate for the baseline control strategy, $\lambda_{baseline}$, can be either obtained from failure rate statistics or can be estimated from a lifetime or degradation model. We further assume that the failure rate for a new control strategy, λ_{CS} , can be calculated by adjusting the baseline failure rate with a failure rate adjustment factor ε :

$$\lambda_{CS} = \varepsilon \cdot \lambda_{baseline} \quad (6)$$

ε is a factor that describes the relative change in number of failures for a new situation compared to a baseline situation. This approach is justified in Appendix C where it is also

extended to a case where the control strategy is applied in a shorter period only (i.e. not over the whole lifetime).

There are different ways to calculate ε . If a degradation model is available, as described before in section 4.1, one can use the degradation model to calculate the influence of both the baseline strategy and the new control strategy on the mean time to failure and estimate the failure rate adjustment factor as follows:

$$\varepsilon = \frac{MTTF_{\text{baseline}}}{MTTF_{\text{CS}}} \quad (7)$$

In section 7.2, another approach is presented that is based on basic relations between wind speed and relative fatigue of mechanical components.

LIFETIME DISTRIBUTION MODEL

In this model, we assume that the component has a stochastic lifetime T that is described by a lifetime distribution, represented by the probability density function $PDF(t|t_S, \mu, \sigma)$, cumulative distribution function $CDF(t|t_S, \mu, \sigma)$ or survivor function $SF(t|t_S, \mu, \sigma)$, where t_S is the time the component already has survived (is in operation), and where μ and σ are the mean and standard deviation of the lifetime distribution.

Note that t is the time since the wind farm was commissioned and that the component was commissioned together with the wind farm at $t = 0$. We also assume that the planned time for usage of the component is t_{WF} . For wind turbines, t_{WF} is usually the lifetime of the wind farm, e.g. 20 years.

The conditional probability of failure Pr_{failure} of the component in the time interval $[t_S, t_{WF}]$, given that the component already has survived until t_S is [7]:

$$\begin{aligned} Pr_{\text{failure}} &= \int_{t_S}^{t_{WF}} PDF(t|t_S, \mu, \sigma) dt = CDF(t_{WF} - t_S|t_S, \mu, \sigma) \\ &= 1 - SF(t_{WF} - t_S|t_S, \mu, \sigma) = 1 - \frac{SF(t_{WF}|\mu, \sigma)}{SF(t_S|\mu, \sigma)} \\ &= 1 - \frac{1 - CDF(t_{WF}|\mu, \sigma)}{1 - CDF(t_S|\mu, \sigma)} \end{aligned} \quad (8)$$

We assume now that a control action increases the average lifetime of the component by Δt , i.e. $\mu_{\text{CS}} = \mu_{\text{baseline}} + \Delta t$. When Δt is negative, the control strategy reduces the expected lifetime of the component. For the sake of convenience, we assume that the standard deviation σ is increased correspondingly, i.e. the shape of the distribution and the coefficient of variation is unchanged. The standard deviation after the control action is:

$$\sigma_{\text{CS}} = \sigma_{\text{baseline}} + \frac{\Delta t}{\mu_{\text{baseline}}} \sigma_{\text{baseline}} = \sigma_{\text{baseline}} \left(1 + \frac{\Delta t}{\mu_{\text{baseline}}} \right) \quad (9)$$

Then, the changed failure probability due to a new control strategy can be calculated as:

$$\Delta Pr_{\text{failure}} = CDF(t_{WF} - t_S|t_S, \mu_{\text{CS}}, \sigma_{\text{CS}}) - CDF(t_{WF} - t_S|t_S, \mu_{\text{baseline}}, \sigma_{\text{baseline}}) \quad (10)$$

$\Delta Pr_{\text{failure}}$ is illustrated in Figure 4-3.

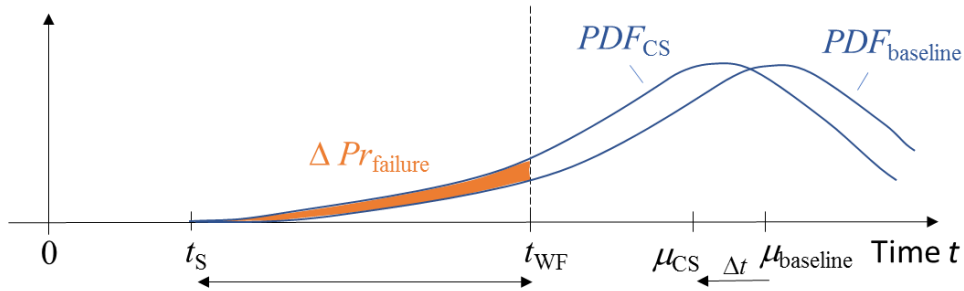


FIGURE 4-3: CHANGED FAILURE PROBABILITY DUE TO CHANGED OPERATIONAL STRATEGY.

Combined with the average cost for corrective maintenance C_{CM} , the influence of the operational action on the corrective maintenance costs is:

$$C_{CS} = \Delta Pr_{failure} \cdot C_{CM} \quad (11)$$

The model requires the following input:

- Lifetime change Δt as a function of a new wind turbine control strategy CS³
- Baseline lifetime distribution for a new component, $F(t|\mu_{baseline}, \sigma_{baseline})$
- Wind farm lifetime⁴, t_{WF}
- Estimate of corrective maintenance cost, C_{CM}

$F(t|\mu_{baseline}, \sigma_{baseline})$ must be established from available statistics or can be estimated based on a failure or degradation model (which e.g. can be used to estimate the mean lifetime). Δt can also be estimated with a failure or degradation model. This is illustrated in Section 6.2 for an example for the transformer.

The model can also be used to calculate the effect of a new control strategy that is not applied over the whole wind farm lifetime, but later in the lifetime, where $t_s > 0$ represents the time the new control strategy is put into operation.

DISCUSSION

Failure rate can refer to two different statistical quantities: 1. The rate of occurrence of failures (ROCOF), which is the average number of failures within a time interval, and 2. the hazard rate, also called force of mortality (FOM), which is the individual (underlying) failure rate for a single component. The hazard rate (FOM) can be interpreted as probability of failure in the next time interval given that the component has survived until time t . We do not further discuss the difference between ROCOF and FOM here, and the reader is referred to Appendix D or [8] [7] for further details.

³ Δt is a function of how long the control strategy is used. Δt is small if the new control strategy is used for only few hours, but larger if the control strategy is used for the whole wind farm lifetime.

⁴ $t_{WF} - t_s$ is the analysis period, i.e. the period for which we want to analyse the effect of a new control strategy on failure probability (and finally costs). The end of the analysis period could also be set to a shorter period than the wind farm lifetime, e.g. to $t_s + \text{one year}$, if one is interested in the benefit and savings in the next year.

The failure rate estimates that are available for wind farm components are usually based on statics about the number of failures for a population of wind turbines observed over a specific time period. This means that these failure rates should rather be used as ROCOF than as FOM. Even though the ROCOF (failure rate) is constant, the underlying component FOM (hazard rate) may not be, especially for components where the time to failure is rather deterministic than random. In these cases, the failure rate model presented above may give quite wrong results in cases where the expected component lifetime is significantly larger than the wind farm lifetime. The examples presented for transformers in section 6.2 and in Appendix D illustrate this problem and show that it might be better to use the lifetime distribution model in such cases. However, the failure rate model is a good model when the hazard rate is constant or close to constant, or when the component lifetime is much shorter than the time period analysed (e.g. the wind farm lifetime).

A drawback of the lifetime distribution model is that the probability of failure that is calculated, is the probability of the first failure. Thus, the model is only valid for cases where we carry out analysis in the left tail of the PDF, see Appendix D for further details and an illustrative example. Thus, the lifetime distribution model should only be used when the contributions to failures and failure costs from second, third, fourth, and so on, failure can be neglected. If the component lifetime is much shorter than the analysis period, one should rather use the failure rate model than the lifetime distribution model, as already discussed above.

A challenge are cases where the analysis period is between 1 and around 3 times the component lifetime. Then one should calculate the ROCOF with the underlying component hazard rate, i.e. the expected number of failures for each time interval in the analysis period, as illustrated by the example in Appendix D. However, this approach is not further described here, because the calculations require usually numerical approaches, such as Monte Carlo simulation.

4.5 PREVENTIVE MAINTENANCE COST MODEL

A changed preventive maintenance strategy is one possibility to respond to increased failure probability resulting from changed operational strategies. One example is to counteract increased failure probability by intensifying preventive maintenance.

This model is based on the assumption that a component requires a major preventive maintenance (PM) task (refurbishment, replacement) after some time interval t_{PM} to keep it running for the next time interval t_{PM} . Assuming that a special control strategy requires that PM must be carried out earlier or later, the time to the next PM task is changed by Δt_{PM} . The additional cost for a new control strategy (compared to the baseline strategy) is given by the difference of the present values (PV) of the PM cost C_{PM} that was moved from t_{PM} to $t_{PM} + \Delta t_{PM}$:

$$\Delta C_{PM} = PV_{\text{baseline}}(C_{PM}) - PV_{\text{CS}}(C_{PM}) = \frac{C_{PM}}{(1+r)^{t_{PM}-t_S+\Delta t_{PM}}} - \frac{C_{PM}}{(1+r)^{t_{PM}-t_S}} \quad (12)$$

r is the discount rate.

The model is illustrated in the figure below:

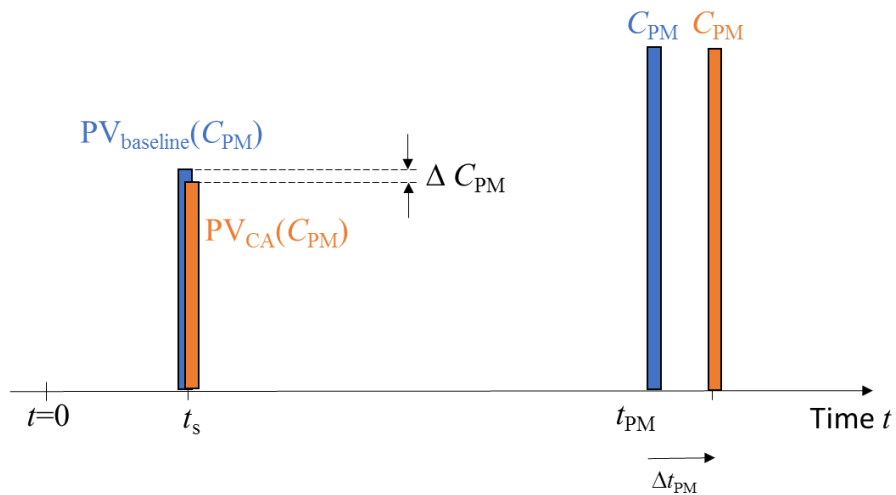


FIGURE 4-4: ILLUSTRATION OF PREVENTIVE MAINTENANCE COST MODEL.

The cost model requires that the relation between turbine control and reduction of next PM time (Δt_{PM}) can be estimated.

The model has been applied to hydropower components to estimate the cost of hydropower unit start-up costs [6] [9]. Hydropower plants have a very long lifetime (100 years and longer). Thus, the assumption is that a preventive maintenance strategy is applied to keep the power plant running for a very long time. The PM strategy consisting of major refurbishments and overhauls that are regularly carried out; e.g. every 5 to 40 years, and can also be a combination of more frequent minor maintenance tasks and less frequent major refurbishments. Then, the strategy is to preventively maintain the components in a "good" condition and avoid corrective maintenance.

ALTERNATIVE PM COST MODELS

Like corrective maintenance, preventive maintenance could also be modelled by a PM rate, i.e. the average number of PM actions per year. The PM rate represents recurrent PM actions such as inspections, and maintenance or replacement of consumables. Then, the PM rate could be adjusted depending on the influence of control on PM, like the failure rate is adjusted, as described in section 4.4.

DISCUSSION

Wind farm components are not maintained according to a strict PM strategy with preventive replacements or refurbishments as components in e.g. hydropower plants. Furthermore, it is unlikely that changed control strategies influence the PM strategy and that maintenance and inspection intervals are changed. Thus, modelling changes in PM costs is unlikely to be a good approach for wind turbines.

Another reason for not using a PM cost model is that the wind farm lifetime is restricted. According to the model, operational strategies that extend the component lifetime would always be beneficial even though they extend the lifetime far beyond the wind farm lifetime. Other forms of discounting (annuities) within the wind farm lifetime and excluding residual values beyond the wind farm lifetime may solve this problem. Nevertheless, due to the mentioned reasons, PM cost models are not further considered in this report.

4.6 DESIGN COST MODEL

A changed control strategy may result in load changes, e.g. reduced (increased) loads that allow for (requires) use of cheaper (more expensive) designs, e.g. by using less (more) material.

A model that relates the load reduction to the mass, cross section and cost reduction has been earlier presented by Chaviropoulos and Natarajan [10]. The load reduction is represented by the load reduction ratio α . The relation between α and the costs/masses/cross sections for a changed operating strategy and the original strategy is:

$$\frac{Cost_2}{Cost_1} = \frac{Mass_2}{Mass_1} = \frac{A_2}{A_1} = \alpha^L \quad (13)$$

L is an exponent that depends on the type of component and which type of loads it is designed for; axial forces, buckling, bending moments, torsion moments. In Section 5, it is outlined how α and L can be calculated for different mechanical components.

DISCUSSION

Load reduction can be directly connected to a reduction in the failure rate/failure probability (as described by the models in section 7.2). When production losses are part of the failure costs, the increased production is given by the reduced failure losses.

Load reduction can also imply an increase in lifetime of the turbines due to reduced fatigue damage for the same design. This increase in lifetime translates to an increase in AEP over the extended lifetime to determine the impact in LCOE reduction. Thus, for a fixed CAPEX, one may reduce OPEX and increase AEP using fatigue damage lowering control mechanisms.

The presented cost model has been developed for mechanical components. However, the basic idea that improved operating strategies could result in cheaper design is general. Further work could focus on how this idea can be applied to electrical components.

4.7 SUMMARY AND DISCUSSION

Several basic cost models have been presented in this section. The choice of the cost model should depend on the application, since the models have different properties and advantages and disadvantages, as discussed above.

The lifetime distribution model and the preventive maintenance cost model require that the age of the components or the time until next preventive maintenance must be known. When such models are used in control applications, it would require that the controller must have the information about time of commissioning and preventive maintenance of wind farm components. This type of information is available from the computerized maintenance management system (CMMS). However, at current stage, it might be too challenging or impractical to track the age of all components by the controller or receive the required information from other systems like the CMMS. Thus, it is more practical to use simpler models that don't require such input. The investment cost model, the failure rate model and the design cost model represent such models.

Applications and examples of the models are illustrated and discussed in the following sections.

5. RELATIVE MODELS FOR MECHANICAL COMPONENTS

Load reductions in one component of the wind turbine such as the blade, may translate into differing reductions of design loads on other connected components, such as the tower. As such a detailed quantification of the impact of such load reductions on the design of structures or damage in structures would require detailed load simulations and iterations, which is too computationally expensive a process to input to cost models. Methods for computing fatigue on different wind turbine mechanical components are described in section 7. Herein the relative benefit in mass or cost due to a reduction in loading is quantified using simple models.

Two complementary basic cost models are suggested for mechanical components, the failure rate model as introduced in Section 4.4 and the design cost model as introduced in Section 4.6. The former is applied to the wind farm model presented in Section 7 and is described in Section 7.2. The latter is presented below.

The following notation is used in this section:

A	Cross section	M	Bending moment
α	Load reduction ratio	R	radius
d	deflection margin ratio	σ_{\max}	Maximum normal stress
F	Axial force	t	Thickness
L	Exponent	W	Bending resistance
$w(x)$	Displacement along a beam		

The following is based on the descriptions in [10].

We assume that the wind turbine structures can be approximated as beam elements whose cross sections can be ideally modelled as thin-wall cylinders of radius R and thickness t . Such a model represents typical steel tower and substructures of an offshore wind turbine, but it may be also used as an abstract representation of the blades or the drive train load carrying components.

Assuming a bending-tension (or compression) load case resulting from a bending moment M and an axial force F , the maximum normal stress in the cross section derives from the formula

$$\sigma_{\max} = \frac{F}{A} + \frac{M}{W} \quad (14)$$

$A = 2\pi R t$ is the cross section area and $W = \pi R^2 t$ its bending resistance. Load reduction can be connected to the expected area reduction by assuming that the maximum stress σ_{\max} remains the same under the different loading conditions. We shall study as two individual cases, the pure axial and the pure bending load cases. Let subscript 1 denote the reference design and subscript 2 the innovative design, the one with the reduced loads.

AXIAL FORCE DRIVEN DESIGNS

If α stands for the load reduction ratio (Load2/Load1) then for the axial load case:

$$\alpha = \frac{F_2}{F_1} = \frac{A_2}{A_1} = \frac{t_2 R_2}{t_1 R_1} \quad (15)$$

which is valid for both tension and compression loads, the latter under the constraint that the local buckling resistance of the section is maintained through a proportional change of the radius and thickness ratios, that is:

$$\frac{t_2}{t_1} = \frac{R_2}{R_1} = \left(\frac{A_2}{A_1}\right)^{\frac{1}{2}} \quad (16)$$

and global buckling is not a failure mode.

M-DRIVEN OR TORSION DRIVEN DESIGNS

For the bending load case, i.e. for F-driven designs, α is:

$$\alpha = \frac{M_2}{M_1} = \frac{W_2}{W_1} = \frac{R_2^2 t_2}{R_1^2 t_1} \quad (17)$$

For maintaining local buckling resistance, we assume that (16) holds and therefore

$$\alpha = \frac{M_2}{M_1} = \frac{R_2^2 t_2}{R_1^2 t_1} = \frac{R_2^3}{R_1^3} = \left(\frac{A_2}{A_1}\right)^{\frac{3}{2}} \quad (18)$$

MAXIMUM DEFLECTION

Utilizing the Euler-Bernoulli beam deflection equation

$$\frac{d^2 w(x)}{dx^2} = \frac{M(x)}{EI(x)} \quad (19)$$

where $w(x)$ is the displacement along the beam axis $M(x)$ is the bending moment and $EI(x)$ the flexural stiffness, one can show based on the above assumptions for buckling resistance that for the reference and innovative designs are interrelated through:

$$d = \frac{w_{2max}}{w_{1max}} = \frac{\alpha}{\left(\frac{A_2}{A_1}\right)^2} \quad (20)$$

with $\alpha = \frac{M_2}{M_1}$, or,

$$\frac{Cost_2}{Cost_1} = \frac{Mass_2}{Mass_1} = \frac{A_2}{A_1} = \left(\frac{\alpha}{d}\right)^{\frac{1}{2}} \quad (21)$$

LOAD REDUCTION IMPACT ON MASS AND COSTS

If the load reduction potential from wind farm control for a specific turbine is uniform along the idealized turbine structure (which can be assumed in this case) then the load reduction impact on mass (and cost) derives from (13) as

$$\frac{Cost_2}{Cost_1} = \frac{Mass_2}{Mass_1} = \frac{A_2}{A_1} = \alpha^L \quad (22)$$

where $L = 1$ for axial force driven designs, $L = \frac{1}{2}$ for deflection limited design and $L = \frac{2}{3}$ for bending moment driven design.

For fatigue dominated designs, the above rules can still be used where the physical load is replaced by the lifetime damage equivalent load.

SUMMARY

Summarizing the above findings in a single table addressing specific wind turbine components we read:

TABLE 5-1: SCALING LAW FROM LOAD REDUCTION TO COMPONENT MASS REDUCTION

Component	Load ratio (α)	Strength	Fatigue	Deflection
<i>Blades</i>	<i>M-driven</i>	$\alpha^{2/3}$		$(\alpha/d)^{1/2}$
<i>Main Shaft</i>	<i>Torsion</i>		$\alpha^{2/3}$	
<i>Tower, monopile</i>	<i>M-driven</i>		$\alpha^{2/3}$	$(\alpha/d)^{1/2}$
<i>Jacket</i>	<i>F-driven</i>		α	-

Assuming that the design in a component is dominated by one of the factors given in the above table, it implies that the mass of the component scales by a factor that can be computed based on the load change; for example, the mass of the support structure changes to the power (2/3) of the relative bending moment change. A load reduction would thereby imply a lifetime increase for the same fatigue damage equivalent load target. This increase in lifetime can be converted to an increase in AEP to determine the impact in LCOE.

For example [11], the offshore support structure is the most expensive component of the turbine and it is also a fatigue design structure. Assuming that the stress in the substructure is bending dominated; then from Table 5.1, it implies that the mass of the substructure scales by a factor of (2/3) of the stress change. For a fixed fatigue S-N curve slope, a 5.5% reduction in bending fatigue stress would thereby imply a 3.5% reduction in the mass of the substructure for meeting the same lifetime target. If the SN curve slope is assumed to be 5 (as in the case of steel), such a reduction in bending fatigue stress of 5.5% can instead also imply a 24% increase in operating lifetime of the support structure, if the mass of the structure were not reduced. This increase in lifetime of the support structure can be translated to increase in AEP, given the prevailing wind conditions and sufficient life of the remaining turbine components.

In terms of the repair/replacement cost of the mechanical components, Table 5-2 provides an approximate indicative figure of the cost of replacement offshore of a mechanical component as a multiple of the material cost of the component for traditional wind turbines less than 5 MW in capacity. This overall replacement cost includes the cost of the vessel, crane and labour on top of the component material cost. More OPEX cost details if required for different components can be obtained from [12]. Table 5-2 also provides an estimated failure rate and the percentage of the overall wind farm OPEX that these mechanical component replacements constitute. The gearbox replacement occupies the most percentage of the wind farm OPEX since its MTBF is low and replacement costly, if done separately for different turbines in a wind farm. The pitch bearing may also have a low MTBF, but it may not be as expensive to replace as a gearbox.

TABLE 5-2: COST OF REPLACEMENT OF MAJOR MECHANICAL COMPONENTS

Components	Overall cost of Replacement (Ratio to material cost)	Failure rate [/year]	Percentage of overall Wind Farm OPEX
Blade	2.1	0.001	2.5%
Gearbox	1.9	0.045	60%
Main shaft with main bearing	2.7	0.003	3%
Pitch Bearing	4.0	0.040	12%

The fraction of the overall OPEX costs at a wind turbine level as represented by these major component replacements is also provided in Table 5.2. These costs would need to be combined with the mean time between failures to ascertain the lifetime costs.

Further details of the implemented cost model is provided in chapter 7 and therefore it is not repeated herein for its impact on mechanical components.

6. MODELS FOR ELECTRICAL COMPONENTS

This chapter presents models for estimating degradation and lifetime of power converters and transformers. The degradation and lifetime models presented result directly in an estimate of the lifetime, remaining lifetime or consumed lifetime.

The estimates of lifetime or consumed lifetime can be used as input to different cost models as already presented in section 4.2, namely the investment cost model and the corrective maintenance cost models. The main focus in this section is on the degradation models. However, selected examples of application of the degradation and lifetime modelling results in cost modelling are included.

For electrical components, we assume that the power production profiles (i.e. power production time series) for the turbines in the wind farm are an input to the electrical component models, that is, we assume them as given. Thus, the models presented in this section answers the question "If the wind turbines in the wind farm will produce power in the next period ⁵ according to the following profile, how much of the lifetime will be consumed?" There are activities in other tasks and work packages in the TotalControl project that deal with modelling the effect of wind farm control on the wind field and the energy yield in the wind farm. These models can be used to estimate the power production profiles.

6.1 POWER CONVERTERS AND POWER CYCLING RELIABILITY

The reliability of power electronics converters is affected by the correct operation of its multiple parts and primarily by the capacitors and switching devices. In this section, the focus is on the reliability of the switching devices and specifically to what referred as power cycling reliability. Indeed, this reliability aspect is heavily affected by the operating conditions and could be modified with control actions. Other failure mechanisms for the semiconductor devices (e.g. failure due to cosmic radiations) are of more random nature and could be marginally dependent or completely independent by control strategy choices.

Failures in power electronics converters can be triggered by repetitive variation of their output power that is conventionally referred to as power cycling. When operating with non-constant current, a semiconductor device (e.g. IGBT module; IGBT: Insulated-gate bipolar transistor) is subjected to changes in its power losses and, consequently, in its internal temperature distribution. These temperature variations may induce thermo-mechanical stress and ultimately breakdown of the device packaging (e.g. bond wire lift-off, solder layer cracking) due to cumulative mechanical fatigue. This section presents the generalities for power cycling reliability and describes a simplified procedure derived from [13] to estimate the expected lifetime for the semiconductor devices in a wind energy conversion system based on field measurement data. Numerical examples are included for a notional 3.67 MW Direct Drive wind turbine exposed to a wind data profile derived from measurements on the Lillgrund windfarm.

⁵ The period length can be chosen quite differently, according to the needs of the application, e.g. next 24 hrs or the whole lifetime. Note that for the converter model, the period length must cover a long enough period that contains a reasonably amount of representative power cycles (e.g one year).

The power cycling lifetime of the semiconductor devices in a power converter can be estimated by applying lifetime models on the expected operating profile. A practical procedure is indicated in the following sequence of steps and summarized in the Figure 6-1:

- Power losses in the component can be estimated from the operating conditions (i.e. voltage and current profiles). These conditions could be obtained by electromagnetic transient simulations on a numerical model of the converter system including its control. The model should account for each switching event so modulation should be modelled in detail (e.g. no simplified average model)
- The internal junction temperature in the component as a function of the time can be predicted by combining these estimated losses with a thermal model of the component. The thermal behaviour of the component is normally represented with a lumped thermal network.
- Due to the aging process, like degradation of solder layers, also the thermal impedance will change by time. Therefore the thermal model should to be updated online. One approach for this is by estimating hotspot temperature by measuring some thermosensitive electrical parameters (TSEP) for the IGBT. Another approach is by running a real time estimator (digital twin) and compare simulated state variables with real measurable variables.
- Since the power cycle lifetime models are normally formulated for elementary repetitive stress cycles, the expected lifetime cannot be directly calculated for a generic temperature profile. A common approach is to decompose arbitrarily complex profiles in discrete elementary cycles and to superimpose their effect. Since degradation is linked to mechanical fatigue, algorithms developed for predicting the fatigue lifetime of mechanical parts appear as the most suitable (i.e. Rainflow counting). Low amplitude temperature cycles (e.g. $< 10\text{ }^{\circ}\text{C}$) not sufficient for inducing plastic deformations should be discarded.
- The reduction of lifetime due to every cycle can be computed from a power cycling lifetime model. Several parametrized power lifetime models are available in the technical literature. In general, model parameters are obtained by fitting experimental data from accelerated destructive tests.
- The effect of the different cycles is superimposed, and their associated damage cumulated. A linear superposition hypothesis is normally adopted (Miner's formula).

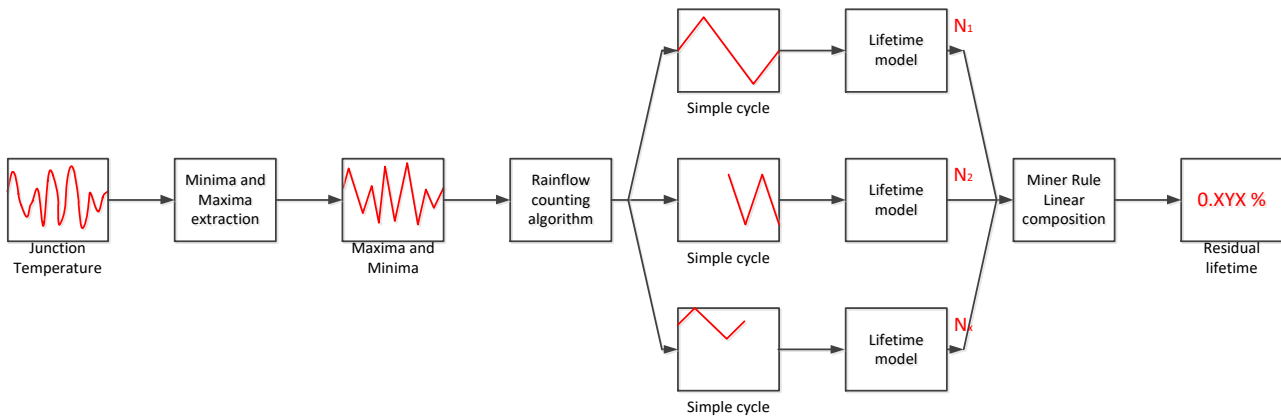


FIGURE 6-1: STEPS FOR ESTIMATING POWER CYCLING LIFETIME OF A POWER MODULE FROM THE VIRTUAL JUNCTION TEMPERATURE PROFILE.

ELECTRICAL SIMULATION AND THERMAL MODEL

The following notation is used for power converter lifetime and reliability modelling:

α	Constant in Coffin-Manson term	n	Counter variable (stress cycles)
β	Parameters in lifetime model	P	Active power
D	Diameter of bonding wire	Q	Reactive power
f	Frequency in electrical grid	t_{on}	Power on time
Ge	Generator side	t	Time
Gr	Grid side	T	Temperature
i	Counter variable	ΔT	Temperature swing
I	Current per bond wire foot	V	Blockage voltage
j	Counter variable	v	Wind speed
k	Boltzmann constant	lr	Lifetime reduction
E_a	Activation energy	T_m	Medium temperature

Power cycling is the result of the thermal stress applied to the device during operation. Consequently, to predict the expected lifetime it is first necessary to calculate the losses and then the virtual junction temperature $T_j(t)$ of the semiconductor devices as function of time for the expected operating conditions. This temperature can be estimated with numerical models or derived by direct measurement. The numerical calculation of the temperature requires mathematical models for the losses and for the thermal propagation in the device. The inputs for these models are the operating conditions of the converter (e.g. phase currents, DC bus voltage) that can be obtained by circuit simulation. Input for the loss calculation can be, for example, the active and reactive power of a wind turbine fed into the grid. Several approaches have been described in literature and often based on well-known and proved simplifications (e.g. the semiconductor characteristic curves are linearized, heat flux is modelled as a Foster-network). A second possibility is to measure the temperature time sequence by monitoring the temperature online (e.g. $V_{CE}(T)$ method according to [14]), thus, minimizing calculation errors

due to model-based simplifications. However, this method is not used in common wind converters due to challenges for the implementation of the measurement circuit into the actual power and control circuit.

CYCLE COUNTING AND DAMAGE SUPERPOSITION

The characterization of materials resistance to mechanical fatigue is normally conducted by testing their lifetime in terms of cycles when subjected to constant amplitude stress reversals. Thus, elementary cycles should be extracted from the junction temperature profile with cycle counting algorithms before applying the lifetime models. At present, the Rainflow algorithm in its variants is the most popular algorithm for cycle counting in mechanical fatigue predictions. The algorithm was originally developed by Endo and Matsuishi in 1968 and was named for the analogy of the cycle counting process with the rainflow on a pagoda roof graphically similar to the stress load rotated 90 degrees as shown in Figure 6-2. Several implementations of the Rainflow algorithm exist in literature including free versions available in the internet for common commercial software as MATLAB®. Due to the strong analogy of the failure mechanism of IGBT modules with the mechanical fatigue, the Rainflow algorithm is routinely applied also to the prediction of power cycling lifetime. The mechanical stress is replaced by the swings on the virtual junction temperature.

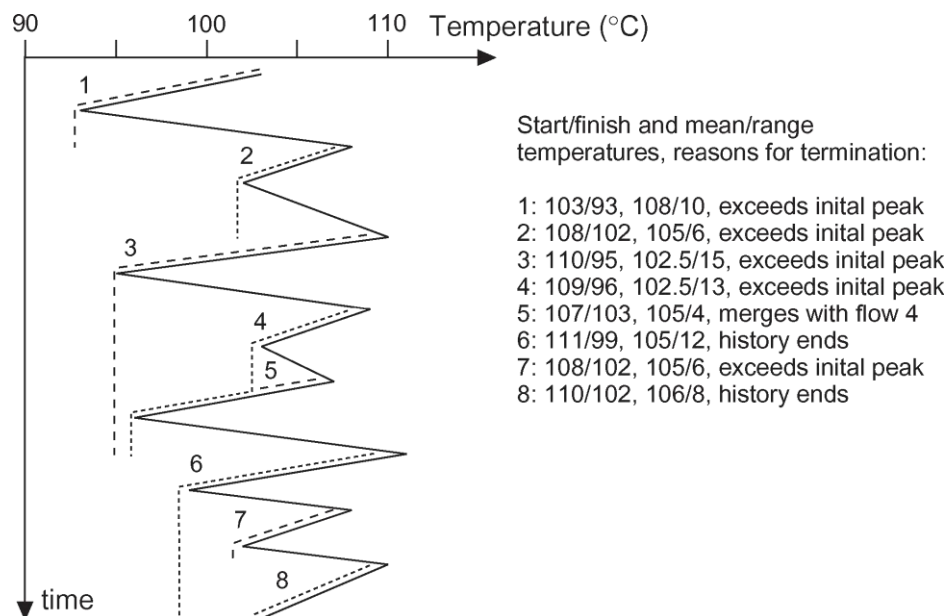


FIGURE 6-2: EXAMPLE OF RAINFLOW COUNTING APPLIED TO TEMPERATURE LOAD [15]. NOTICE THE ANALOGY OF THE CYCLE COUNTING WITH THE RAINFLOWS (DOTTED LINES).

The Rainflow counting operates on the peaks and valleys of the loading profile so the temperature profile could be simplified by extracting and processing only the relative minima and maxima. Small amplitude cycles should be discarded since they would induce only elastic deformations with a negligible effect to the lifetime. Thus, computational efforts required by the cycle counting algorithm can be reduced by discarding in advance the maxima and minima associated to cycles whose amplitude is lower than a set threshold in a range of several degrees Celsius (e.g. 10 °C).

The combined effect of these cycles should be cumulated to estimate the lifetime associated to the temperature profile. A conventional approach to combine the contributing cycles is a linear superposition also referred to as Miner's rule (Palmgren-Miner linear damage hypothesis). This is equivalent to assume that if a repetitive stress leading to failure of the component in N cycles is applied for n times, the associated reduction of lifetime is equal to:

$$lr = \frac{n}{N} \quad (23)$$

The cumulated effect of multiple cycles is obtained by adding the single contributions as:

$$LR = \sum_{i=1}^k \frac{n_i}{N_i} \quad (24)$$

Failure of the component is predicted when this cumulated fraction equals to unity. The linear superposition is a strong simplifying assumption and introduces a degree of uncertainty. Indeed, experimental tests for mechanical fatigue proved that combining the effect of cycles can introduce deviations and failure can occur when the cumulated fraction ranges between 0.7 and 2.2. The degree of inaccuracy of this simplification on power cycling lifetime estimation in power electronics converters has not been well characterized yet in literature.

LIFETIME CHARACTERISTICS

The lifetime consumption corresponding to each cycle is commonly computed based on lifetime characteristic curves. These lifetime curves, referring to special types of semiconductor devices, are the result of more or less standardized power cycling tests. In literature different models for lifetime estimation of power modules are available when subjected to repetitive power cycling. These models normally incorporate an Arrhenius term representing the effect from the average temperature, and a Coffin-Manson term that introduces an exponential dependence with the temperature swing:

$$N_f = a (\Delta T_j)^{-n} e^{\frac{E_a}{k T_m}} \quad (25)$$

where ΔT_j is the temperature swing, T_m is the junction medium temperature, k is Boltzmann constant, E_a represents the activation energy, and a and n are two constants to be obtained by experimental measurements. This model is in the literature often referred to as the Lesit model.

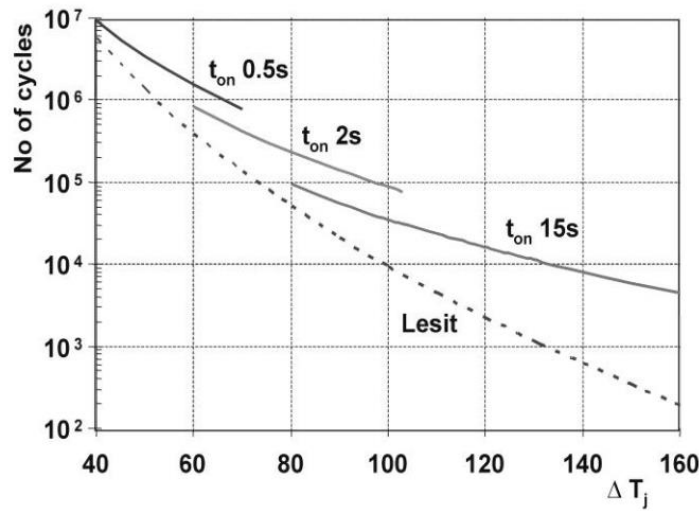


FIGURE 6-3: EXAMPLE OF LIFETIME CURVES FOR THE CIPS 2008 MODEL [16]

The model represents the lifetime of the module as:

$$N_f = k \Delta T_j^{\beta_1} \cdot e^{\frac{\beta_2}{T_j + 273}} \cdot t_{on}^{\beta_3} \cdot I^{\beta_4} \cdot V^{\beta_5} \cdot D^{\beta_6} \quad (26)$$

where k and β are constant parameters (β_3 to β_6 are negative), t_{on} is the power on time, V is the blocking voltage of the chip, D is the diameter of the bonding wire, I the current per bond wire foot.

MATLAB IMPLEMENTATION OF LIFETIME ESTIMATION WITH SIMPLIFIED CYCLE COUNTING

Junction temperature profiles for a wind energy conversion system contain both low frequency components with large amplitude cycles due to the variations in the wind speed and high frequency components with small amplitude cycles at the ac electrical frequency. These high frequency oscillations are due to the sinusoidal current flowing into the converter legs and are present also in steady state conditions. The presence of these two temperature variations spectra quite distinct in the frequency domain allows to account them separately and merging their effect in a later stage with the Miner rule.

The lower frequency oscillations are linked to the fluctuations of the wind and large variations in the output power production. The relatively slow dynamic of the wind variations allows sampling the wind data also with a time resolution of several minutes without significantly affecting the overall accuracy of the results. Since the longest thermal time constant for a typical power module is in the range of several seconds, the system dynamic can be assumed as a sequence of steady state conditions. The steady state behaviour of the wind turbine can be characterized by executing a batch of numerical simulations of the combined electrical and thermal model with constant external conditions. For simplicity, it will be assumed that the steady state conditions are depending only by the wind speed; the effect of other external conditions with a minor relevance as the grid voltage or the ambient temperature is neglected. Thus, the temperature conditions and main electrical variables can be mapped as function of wind speed v :

- Active power $P(v)$
- Reactive power $Q(v)$

- Frequency steady state temperature oscillations $f(v)$
- Minimum temperature IGBT $T_{IGBT,min}(v)$
- Maximum temperature IGBT $T_{IGBT,max}(v)$
- Maximum current $I(v)$

In order to reduce the computational effort of this characterization, a limited number of wind speeds can be simulated and the functions for intermediate wind speed values can be derived by interpolation. Alternatively, these functions can be expressed also in terms of P by inverting the first function. The mapping allows to determine the temperature components as a function of the produced power or wind speed profile and to apply the steps explained in the previous subsections (cycle counting, estimation damage for cycle components and linear superposition of damage).

NUMERICAL EXAMPLE ON A CASE BASED ON LILLGRUND POWER PRODUCTION PROFILE

In this numerical example, power cycle lifetime is calculated for a windfarm consisting of 3.67 MW wind turbines as in [13] but with a production profile based from data for the Lillgrund. The power production profile for one of the 46 turbines considered is displayed in Figure 6-4.

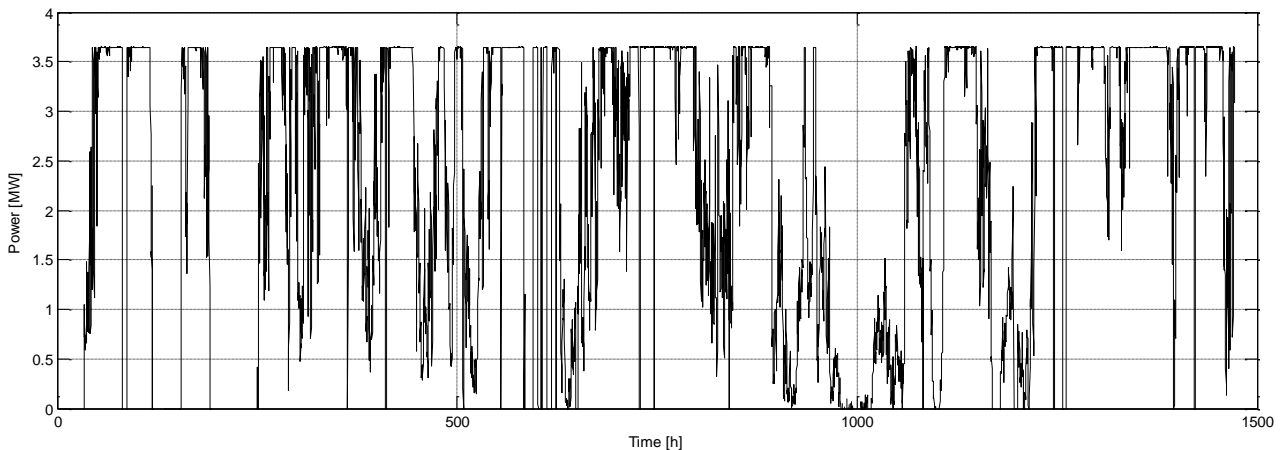


FIGURE 6-4: POWER PRODUCTION PROFILE FOR ONE OF THE 46 TURBINES CONSIDERED

The differences in the rated power has been accounted by scaling the profile by the ratio of the nominal powers between the reference turbine and the turbines in Lillgrund. The mapping functions with input from the wind speed are reported in Table 6.1 below for the grid side (GR) and the generator side (GE) converters. Ambient temperature has been assumed constant and equal to 25°C. The converter design is based on the two parallel modules Infineon 6MS300R17IE4-3WAH-B10C18VT rated at 1700 DC, 1800 Arms (2.7 MVA three phase). Each valve of the VSC is designed by paralleling three Infineon FF1000R17IE4 IGBTs.

TABLE 6-1: SUMMARY OF STEADY STATE CONDITIONS.

w	f_{Ge}	I_{Ge}	$T_{IGBTmax,Ge}$	$T_{IGBTmin,Ge}$	f_{Gr}	I_{Gr}	$T_{IGBTmax,Gr}$	$T_{IGBTmin,Gr}$
[m/s]	[Hz]	[A]	[°C]	[°C]	[Hz]	[A]	[°C]	[°C]
5	7.1	186.5	37.8	33.5	50	159.0	35.5	34.0
6	8.7	269.2	44.6	38.6	50	178.0	38.0	36.0

7	10.3	372.1	52.6	45.0	50	230.2	43.0	40.0
8	11.9	489.4	61.5	52.2	50	304.7	50.4	45.7
9	13.6	617.1	71.4	60.1	50	404.9	59.8	52.8
10	15.2	758.8	82.5	69.2	50	532.3	71.7	62.2
11	16.8	843.6	89.3	75.0	50	644.9	82.8	70.8
12	18.4	863.1	90.9	76.4	50	680.2	86.8	73.8
13	20.0	864.8	91.0	76.5	50	687.3	87.4	74.3

The steady state minimum and maximum and average virtual junction temperature for IGBTs on the grid side and generator side converters as function of the power are displayed in the Figure 6-5:

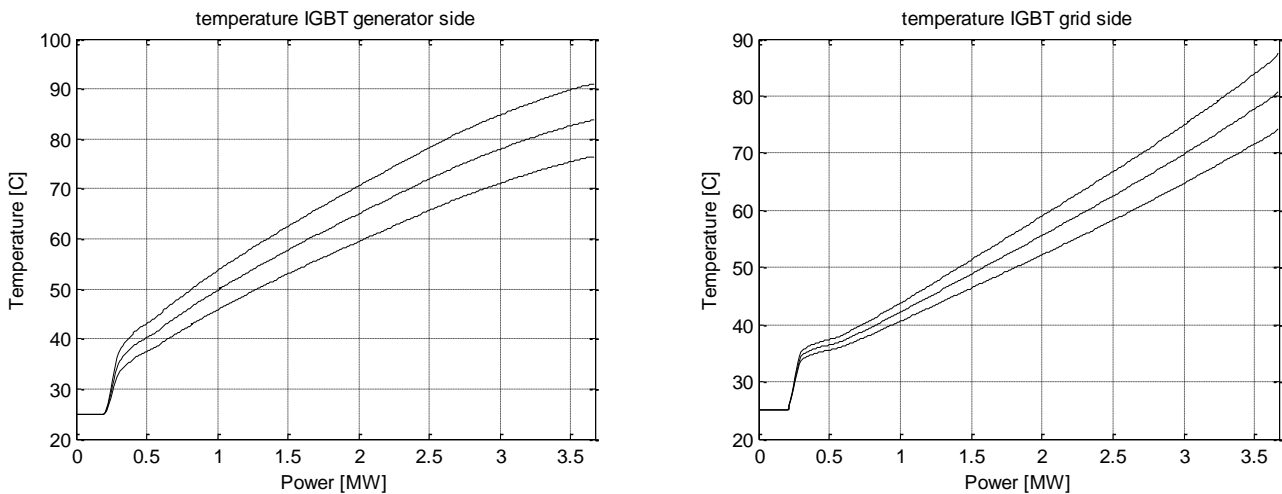


FIGURE 6-5: STEADY STATE MINIMUM AND MAXIMUM AND AVERAGE VIRTUAL JUNCTION TEMPERATURE FOR IGBTs ON THE GRID SIDE AND GENERATOR SIDE CONVERTERS

By combining the static characteristics displayed above with the power production profiles for the turbines the associated virtual junction profile can be obtained. In Figure 6-6, the average virtual junction profile corresponding to the power profile reported in Figure 6-4 is provided.

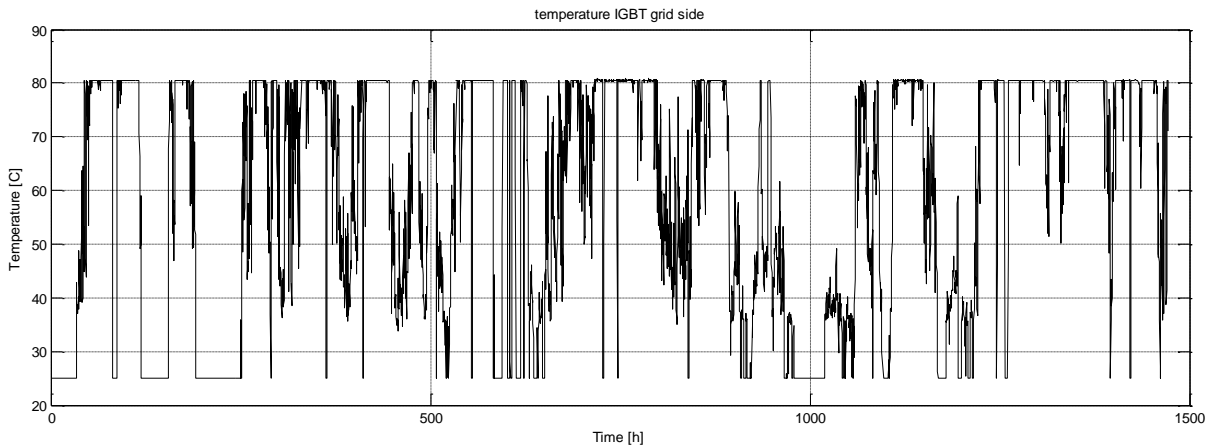


FIGURE 6-6: AVERAGE VIRTUAL JUNCTION PROFILE FOR ONE OF THE TURBINES CONSIDERED

In the lifetime equation, the parameters from the CIPS 2008 publication [16] have been used:

$$a = 9.30 \cdot 10^{-14}; V = 12; D = 300; \beta_1 = -4.416; \beta_2 = 1285;$$

$$\beta_3 = -0.463; \beta_4 = -0.716; \beta_5 = -0.761; \beta_6 = -0.5; N_{bw} = 96$$

The expected lifetime for the IGBT on the grid side and converter side in each of the turbines is displayed in the bar plot in Figure 6-7. It should be considered that the lifetime is very dependent on the threshold assumed as limit between plastic and elastic deformation. In the case it has been assumed a threshold of 15 °C. However, if the threshold is reduced to 10 °C the lifetime is heavily affected. This parameter is difficult to derive, and a model calibration based on historical failure data is recommended before setting its value.

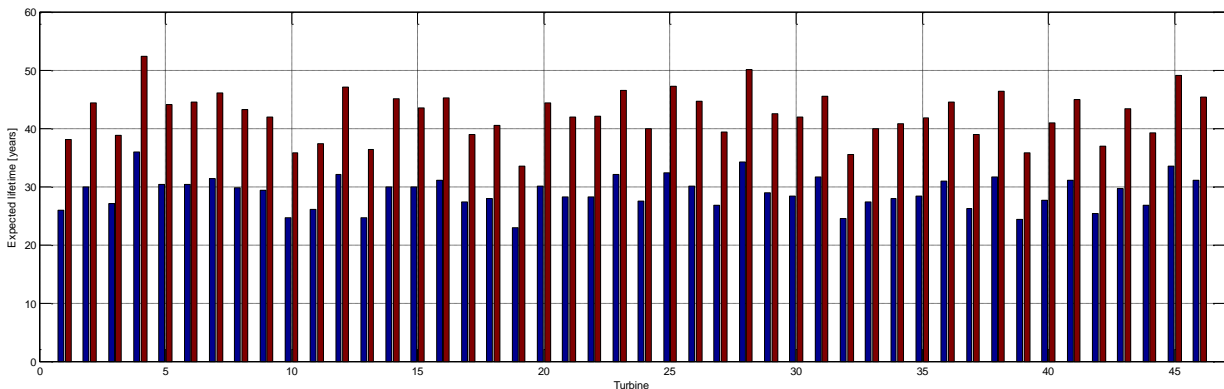


FIGURE 6-7: EXPECTED LIFETIME FOR THE IGBT ON THE GRID SIDE (RED) AND GENERATOR SIDE (BLUE) IN EACH OF THE TURBINES.

INFLUENCE OF CONTROL ON IGBT LIFETIME AND COST

The influence of control on the converter lifetime is illustrated in Figure 6-8. We can see that lifetime for the IGBT on the grid side (red bars) is increasing with derating. However, the lifetime of the IGBT on the generator side (blue bars) is less influenced.

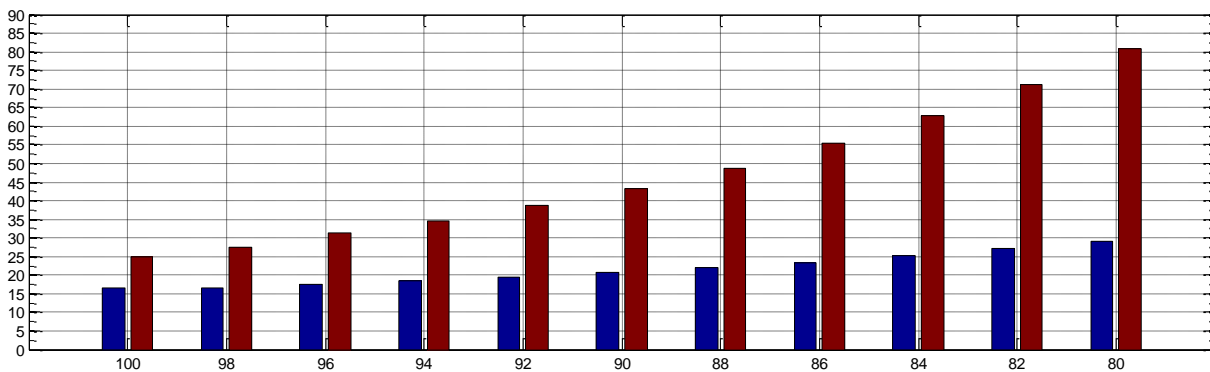


FIGURE 6-8: INFLUENCE OF CONTROL ON IGBT LIFETIME, WHERE 1 REPRESENTS THE BASELINE (NO DERATING, 0%) AND 2-11 STRATEGIES WITH INCREASING DERATING (2-20% DERATING, INCREASING IN 2% STEPS). BLUE: GENERATOR SIDE, RED: GRID SIDE.

The results presented above can be used as input in different cost models. For example, one could use the inverse of the estimated converter lifetime as failure rate for the failure rate cost model (Section 4.4). Then, the inverse of the converter lifetime for the baseline situation would be the baseline failure rate, and the inverse of the lifetime for situations with derating, would be the failure rate influenced by control. In this way, the results could be used in the wind farm cost model as presented in Section 7.

Note that the converter lifetime, or the contribution to lifetime that can be influenced by converter operation and control, is quite deterministic. Thus, the failure rate model might not be the most appropriate one for the converters. Alternatively, one could use a lifetime distribution model (4.4) similar to the one presented for the transformer in the next section.

The converter results could also be used for the investment cost model (Section 4.3). If, for example, $lt(100)$ is the lifetime for 0% derating, and $lt(80)$ the lifetime for 20% derating, $1/lt(100)$ and $1/lt(80)$, respectively, are the parts of the lifetime that are consumed (or written-off) from the investment cost in one year of converter operation. Since there are several IGBTs in one converter, one must estimate which part of the converter investment cost one would relate to one IGBT.

6.2 TRANSFORMERS

For the transformer, the lifetime is much dominated by the condition and degradation of the winding insulation material. Traditionally, power transformers are insulated with cellulose paper (e.g. Kraft paper) and mineral oil. The main substation transformer in wind farms are hence expected to be of this type. For example, this is the case at the Lillgrund wind power plant [17], where the main substation transformer is of the traditional ONAN (oil natural, air natural cooling system) type with paper and oil insulation.

Due to space constraints and high loading during strong winds, turbine transformers are typically not of the traditional cellulose-oil insulated type. Instead, turbine transformers have a compact design using materials that can better withstand high loads and hence high internal temperatures. For example, at Lillgrund, turbine transformers are filled with silicon liquid with a high fire point (above 360°C). These transformers are manufactured by Pauwels. Siemens use Nomex insulation material together with synthetic ester oil in their wind turbine transformers. According to Siemens this has been the case at least for the last 10 years. As Siemens is the world leading supplier of wind turbines, this design is expected to be representative of many turbine transformers.

In the following, degradation models are discussed for both turbine and substation transformers. Although there may be only one substation transformer in a wind park, it can still be relevant to include it in a cost model, as the transformer is critical for the entire wind park. For example, at Lillgrund there is no back-up transformer, possibly resulting in a long outage of the entire wind farm in case of transformer break down.

The following notation is used in this section:

DP	Degree of polymerization	$w_{p,hs}$	Concentration of water in the paper at the hot-spot
A	Environment factor in degradation model	$w_{o,hs}$	Water content in the oil at the hot spot
E_a	Activation energy in degradation model	t	Time
R	The universal gas constant	Δt	Time interval
T	Temperature	t_S	Time transformer has survived
T_{hs}	Hot-spot temperature	$t_{baseline}$	Transformer lifetime for the reference case
T_{hs}^*	Equivalent constant hot-spot temperature (defined as the constant temperature that gives the same aging as the full temperature data series)	t_{CS}	Transformer lifetime with control strategy CS
T_a	Ambient temperature	t_{WF}	Wind farm lifetime
ΔT_{to-a}	Top oil temperature rise above ambient temperature at rated load	λ	Transformer failure rate
N	Total number of data points in the hot spot temperature series,	$\lambda_{baseline}$	Transformer failure rate for the reference case
$P(T_{hs,n})$	Probability for occurrence for each data point in the hot-spot temperature series	λ_{CS}	Transformer failure rate with control strategy CS
H	Hot-spot factor	ε	Failure rate adjustment factor
g_r	Average winding temperature rise above average oil temperature at rated load	CDF	Cumulative lifetime distribution function
K	Load factor (load current/rated current)	μ	Mean value of distribution function
R	Ratio of load losses at rated current to no-load losses	σ	Standard deviation of distribution function
x	Oil exponent	$P_{failure}$	Probability of failure
y	Winding exponent	C_{CS}	Cost of a control strategy
O	Multiplication factor for the presence of oxygen	C_{CM}	Corrective maintenance cost

TURBINE TRANSFORMERS

In this project it was not possible to acquire actual design data for turbine transformers. As an example, the following discussion therefore takes general information about Siemens turbine

transformer design (Nomex insulation material with synthetic ester oil) as the starting point, since Siemens is the world leading supplier of wind turbines.

Nomex is an aramid polymer made by DuPont that is commonly used to enable small sized and low weight transformers, or used in highly loaded transformers, as Nomex can withstand high temperatures and does not absorb much water. For comparison, cellulose is cheaper but absorbs significantly more water - as the temperature increases the water is released from the cellulose to the oil, which at emergency overloads possible can result in detrimental water vapor bubbles in the oil. Nomex is produced in several different types. Nomex is designed to withstand high temperatures and is commonly used in flame resistant clothing. The data sheet for Nomex 410 claims that Nomex retains its mechanical and dielectric strength well under long time exposure to high temperatures ($> 220^{\circ}\text{C}$) [18].

In the following, Nomex aging is discussed to see if aging of Nomex can be included in the TotalControl cost model. Nomex aging models are not as evolved as aging models for cellulose, and there are no generally accepted models. However, some accelerated aging tests have been carried out, indicating that Nomex ages slower than cellulose [19] [20] [21]. See e.g. Ref. [14] for a comparison of the reduction of tensile strength for cellulose, Nomex and hybrid cellulose/Nomex in mineral oil during accelerated aging tests. Ref. [14] also indicates that the reduction of oil dielectric strength only to a little extent depends on the type of insulation paper used (cellulose, Nomex and hybrid cellulose/Nomex).

IEC 60076-14 [22] discusses in general terms loading and aging of liquid immersed power transformers with high-temperature insulation materials, such as thermally upgraded cellulose paper and ester liquid. This reference suggests a typical thermal class⁶ of 220 for aramid, as compared to 105 for regular cellulose paper. Furthermore, it is discussed that ester oil reduces the aging of cellulose paper as compared to regular mineral oil.

Wen et al. [23] and Song et al. [24] investigated accelerated aging of Nomex (Song et al. used Nomex 410) in air (i.e. dry transformers) by measuring DP. They concluded that the aging characteristics are similar to the characteristics for cellulose, and that a degradation model in terms of DP similar to the degradation model for Kraft cellulose paper can reflect the aging. However, the method they used for measuring DP involved dissolving Nomex in sulfuric acid, which is not a generally accepted method as of today.

Ranga et al. [25] investigated accelerated aging of Nomex 910 in mineral oil, as well as aging of thermally upgraded Kraft paper (cellulose) but did not measure DP directly. Instead they measured the concentration of furfural - a known aging marker - from which DP can be estimated. Although the relationship between furfural content and DP is known to be uncertain, they concluded that Nomex ages more slowly than thermally upgraded Kraft paper.

Shuhang [26] investigated accelerated aging of Nomex T910 in natural ester. Comparing the results to aging of Kraft paper, they showed that Nomex retains its tensile strength much better than Kraft, although the duration of the experiment was limited (720 hours).

⁶ IEC 60076-14 refers to the thermal class as the maximum service temperature that the user of the material finds appropriate, taking into account the required lifetime of the transformer where the material is going to be used

The above studies are all carried out at temperatures well above normal operating temperatures for a limited time. Also, no aging studies for Nomex immersed in synthetic ester oil has been found. Hence, in conclusion, there are limited aging studies available for Nomex, and no accepted aging model has been identified in the literature. However, the available studies suggest that the aging is slow as compared to cellulose paper. Therefore, if very high transformer temperatures are avoided, the turbine transformer can probably be kept in service for a long time. This conclusion is supported by available statistics showing that the rate of major failures of turbine transformers is very low compared to the rate of major failures of other turbine components [1]. Note however that the above discussion is based on a very limited literature search and does not investigate different types of insulation materials in turbine transformers.

In conclusion, it is not possible to establish an aging model for turbine transformers with realistic parameters. This is partly due to the currently limited research on such aging models, and the lack of transformer design data in this project. The above discussion however indicates that for Nomex, an aging model in terms of the Nomex' DP-value analogous to the established aging model for cellulose paper can be established, as suggested by Wen et al. [23] and Song et al. [24]. In the following, we will therefore describe the aging model for traditional power transformers insulated with cellulose paper and mineral oil, which is a suitable model for the wind farm substation transformer. This model will then be utilized in a degradation cost model for the substation transformer. Furthermore, for illustration purposes, we will apply this aging and cost model also for the turbine transformers, using data for cellulose paper. This is done with the understanding that the model must be updated and verified with realistic data, including actual transformer design data, before it is further used. This includes also acquiring transformer or ambient temperature data from operation, which is necessary input to the aging model, but was not available in this project.

TRANSFORMER DEGRADATION MODEL

For traditional power transformers insulated with cellulose paper (e.g. Kraft paper) and mineral oil, the insulation paper is regarded to be the main limiting factor for the transformer lifetime. There has been substantial research on the aging of such paper, and there are established models for estimating the aging based on the loading of the transformer. Aging is commonly expressed in terms of the cellulose degree of polymerization (DP), which determines the mechanical strength of the paper, and hence the transformers ability to withstand strains. The dielectric performance of the paper is also affected by aging, but to a lesser extent. The aging is largely governed by the temperature inside the transformer, which again is governed by the loading and the ambient temperature or the cooling of the transformer. Hence, the aging is dominated by the periods where the transformer is highly loaded combined with a high ambient temperature. A recipe for calculating this aging is given below based on ref. [27].

The insulation paper in transformer windings degrades over time due to the cellulose molecules decomposing to shorter molecules. The length of the molecules can be expressed as a degree of polymerization (DP), which is the average number of monosaccharide units in the molecules. Insulation with short molecules have less mechanical strength, and hence is more prone to failure if the transformer is exposed to mechanical stress such as due to a short-circuit. A DP-value of 200 is commonly taken as the end-of-life criterion for the paper and thus the transformer. The DP-value can be measured in a laboratory, but this requires a paper sample to be taken from the windings, which is usually not feasible. Therefore, estimating the

DP-value based on the historic loading of the transformer is desirable. The change in the DP from an arbitrary startpoint to an arbitrary endpoint is described by the Arrhenius equation [28]

$$\frac{1}{DP_{\text{end}}} - \frac{1}{DP_{\text{start}}} = \int_{\text{start}}^{\text{end}} dt A(t)e^{-E_a/RT(t)} \quad (27)$$

where DP_{start} and DP_{end} are the DP-values at the start and endpoints, t is the time, $A(t)$ is an environment factor that depends on the moisture and oxygen content in the oil, E_a is the activation energy, R is the universal gas constant, and $T(t)$ is the temperature to which the paper is exposed, which depends on the load. The parameters $A(t)$ and E_a are not independent and have been estimated in laboratory experiments both for standard Kraft paper and thermally upgraded Insuldur paper [28]. In this report,

(27) will be used to calculate the DP-value today (i.e. DP_{end}) from the DP-value when the transformer was commissioned, which typically is around 1000. A discretization of (27) into hours is sufficient, as in this way daily temperature variations are included.

There are typically strong temperature gradients in transformers, and from

(27) this causes also the DP-value to vary within the transformer. For condition monitoring purposes it is desirable to estimate the DP-value at the location in the transformer where the paper degrades fastest, i.e. at the winding temperature hot-spot. For some new transformers, the hot-spot temperature is measured using fibre-optic sensors. In this case, this temperature may be used directly in

(27). For older transformers the hot-spot temperature must be estimated from other temperature measurements such as top oil temperature or ambient temperature (temperature of the cooling medium). Using the IEC temperature model [29], while assuming that the load varies slowly enough that the transformer is approximately in steady state, the hot-spot temperature T_{hs} is given by

$$T_{hs} = T_a + \Delta T_{to-a} \left(\frac{1 + LK^2}{1 + L} \right)^x + H g_r K^y \quad (28)$$

in terms of the ambient temperature T_a . Here ΔT_{to-a} is the top oil temperature rise above ambient temperature at rated load, H is the hot-spot factor, g_r is the average winding temperature rise above average oil temperature at rated load, K is the load factor (load current/rated current), L is the ratio of load losses at rated current to no-load losses, and x and y are the oil and winding exponents, respectively. If the top oil temperature is measured, this is substituted for the sum of the first and second terms on the right side of (28). The constants in (28) can be found from the transformer's temperature rise test and depend on the cooling mode of the transformer (e.g. ONAN, ONAF etc., according to the IEC nomenclature). Note that the assumption of steady state for the temperature in the transformer is often not met, but this simplification enables an approximate estimate of DP to be made from available data.

The activation energy E_a is determined by the paper type and reads 111 kJ for standard Kraft paper ("K") and 86 kJ for thermally upgraded Insuldur paper ("TU") [28]. The environment factor A can be estimated as [28]

$$A = \begin{cases} 4 \cdot 10^8 w_{p,hs} \cdot O & (K) \\ (1.3 \cdot 10^4 w_{p,hs} + 14000) \cdot O & (TU) \end{cases} \quad (29)$$

for standard and upgraded paper, respectively. Here O is a multiplication factor for the presence of oxygen and $w_{p,hs}$ is the concentration of water in the paper at the hot-spot. For transformers with open conservators, O has been estimated to 2 [28]. In the absence of data for other type of conservators, this value will here conservatively be used for all transformers. Assuming moisture equilibrium between the insulation oil and the paper, $w_{p,hs}$ is given by [28] [30]

$$w_{p,hs} = (w_{o,hs} \cdot 2.24e^{-0.04 \cdot (T_{hs}-273)})^{0.63} \quad (30)$$

where $w_{o,hs}$ is the water content in the oil at the hot spot. As the rate of circulation of oil in the transformer is high relative to the rate of diffusion of water between oil and paper, the water content in the oil can be assumed to be approximately the same everywhere. The water content measured in oil samples taken periodically may therefore be used for $w_{o,hs}$ in (29), even though such samples typically are taken from the transformer tank bottom and not from the hot spot. Using data from all historic oil samples, $w_{p,hs}$ can be estimated as a function of time for the entire lifetime of the transformer by linear regression. Alternatively, for some new transformers, $w_{p,hs}$ can be estimated from online relative humidity sensors installed in the oil flow. This is expected to be more accurate, since the underlying assumption of moisture equilibrium in (30) is questionable. For example, at Lillgrund wind power plant, the substation transformer is equipped with such sensors.

TRANSFORMER COST MODEL: FAILURE RATE MODEL

In the following, the above degradation model is used to establish a degradation cost model for transformers, that can be used to assess the cost of control strategies. The model is set up using the failure rate model described in section 4.4, with the following limitations and assumptions:

- The cost model is established to assess control strategies for the entire wind farm lifetime. The model may be adjusted to apply to shorter periods if needed.
- The transformer is taken as a repairable/exchangeable component.
- Due to lack of data, the aging calculation is not based on a full time series of power and ambient temperature, but instead on yearly probability distributions. Although incorrect, it is assumed that there is no correlation between the power (given by the wind strength) and the ambient temperature. This is expected to add some conservatism to the results.
- The power and ambient temperature distributions are assumed to be the same every year. The average of the A-factor in the aging model throughout the transformer lifetime is for simplicity assumed to be independent of the control strategy. This is strictly not correct, but the error is small for control strategies that do not dramatically change the lifetime

From equation (27) and the above assumptions, the DP value after some time period Δt (in hours), DP_{after} , can be calculated by

$$\begin{aligned}
 DP_{\text{after}} &= \frac{DP_{\text{before}}}{1 + DP_{\text{before}} \int A(t) e^{-E_a/RT_{hs}(t)} dt} \\
 &\approx \frac{DP_{\text{before}}}{1 + DP_{\text{before}} \bar{A} \Delta t \sum_{n=1}^N P(T_{hs,n}) e^{-E_a/RT_{hs,n}}}, \quad (31)
 \end{aligned}$$

where DP_{before} is the DP value at the beginning of the time period, $T_{hs,n}$ is element n of the predicted/assumed hot-spot temperature data series during Δt , N is the total number of data points in the hot spot temperature series, $P(T_{hs,n})$ is the probability for occurrence for each data point (normalised so that the sum over the probabilities is 1), and \bar{A} is the average environment factor during Δt . Instead of a time series, here a simplified hot-spot temperature series is calculated from the yearly turbine power distribution and ambient temperature distribution, assuming these two distributions are uncorrelated. Alternatively, and better, the hot-spot temperature time series may be predicted by machine learning algorithms if such a model has been established and trained based on historic load and temperature time series.

Equation (31) can be written in a simpler way as

$$DP_{\text{after}} = \frac{DP_{\text{before}}}{1 + DP_{\text{before}} \bar{A} \Delta t e^{-\frac{E_A}{RT_{hs}^*}}} \approx DP_{\text{before}} \left(1 - DP_{\text{before}} \Delta t \bar{A} e^{-\frac{E_A}{RT_{hs}^*}} \right) \quad (32)$$

The latter simplification is only valid for control actions of very short duration compared to the transformer lifetime, and not used further here. T_{hs}^* is defined as the constant temperature that gives the same aging as the full temperature data series (the equivalent constant hot-spot temperature):

$$T_{hs}^* = \frac{-\frac{E_A}{R}}{\ln \sum_{n=1}^N P(T_{hs,n}) e^{-\frac{E_A}{RT_{hs,n}}}} \quad (33)$$

Rearranging equation (32), it can also be used to estimate the total expected lifetime t_{CS} when the control strategy CS is applied throughout the lifetime:

$$t_{CS} \approx \frac{DP_0 - DP_{\text{end}}}{DP_0 DP_{\text{end}} \bar{A}} e^{\frac{E_A}{RT_{hs}^*}} \quad (34)$$

where DP_0 is the DP-value when the transformer was new, DP_{end} is the end-of-life criterion, and T_{hs}^* is the equivalent hot-spot temperature resulting from the control strategy. $DP_0=1000$ and $DP_{\text{end}}=200$ are common values for cellulose paper. (32) is a simplified equation, since in reality \bar{A} depends on t_{CS} . However, here it is assumed that \bar{A} may be reasonably well estimated without knowing t_{CS} explicitly. Also, it is not expected that \bar{A} will change a lot with the control actions, and it is the relative change in lifetime due to control actions that is the subject of interest here.

When establishing the cost model it is convenient to define a reference case, denoted "baseline" (see section 4.1), which results in an expected lifetime t_{baseline} (as given by the end-of-life value DP_{end}). From equation (34), the failure rate adjustment factor from section 4.4 can then be found as:

$$\varepsilon = \frac{\lambda_{CS}}{\lambda_{\text{baseline}}} = \frac{t_{\text{baseline}}}{t_{CS}} = e^{\frac{EA}{R} \left(\frac{1}{T_{hs, \text{baseline}}^*} - \frac{1}{T_{hs}^*} \right)} \quad (35)$$

where $T_{hs, \text{baseline}}^*$ is the equivalent constant hot-spot temperature in the reference case, and the assumption that the inverse of the transformer lifetime can be interpreted as an average failure rate λ has been used. Applying the corrective maintenance failure rate cost model from section 4.4, the cost of a control strategy C_{CS} that is applied throughout the transformer lifetime can then be found as

$$C_{CS} = \varepsilon \lambda_{\text{baseline}} t_{\text{wf}} C_{CM} = \frac{t_{\text{wf}}}{t_{CS}} C_{CM} \quad (36)$$

Here t_{wf} is the expected wind farm lifetime and C_{CM} is the cost of corrective maintenance. In the latter step the cost is rewritten to be presented in terms of the investment cost model, which in this case is an equivalent model.

This model has been implemented in an Excel tool, integrated with the model presented in section 7. In this case, the model has been implemented for turbine transformers for illustration purposes only. In lack of model and design data for the materials in turbine transformers, data for cellulose-insulated transformers has been used. The implementation however illustrates well the use of the model.

TRANSFORMER COST MODEL: LIFETIME DISTRIBUTION MODEL

Here the above degradation model is used to establish an alternative degradation cost model for transformers in terms of the lifetime distribution model described in section 4.4.

The above cost model based on failure rates has the disadvantage that there is no time dependence, i.e. the failure rate is constant. This results in an over-estimation of the probability of failure when the transformer is young. The lifetime distribution cost model constitutes a model that can take such time dependency into account, such that the probability of failure increases when the transformer becomes degraded. However, this model requires that a lifetime distribution for the transformer is established from some statistics or other means. Furthermore, this distribution must be updated individually for each transformer based on the control strategy, as explained in section 4.4.

From section 4.4, the cost of a control strategy CS put in effect from the time t_S to the end of the wind park lifetime t_{WF} is in this model given by

$$C_{CS} = Pr_{\text{failure}} \cdot C_{CM} \quad (37)$$

Here the conditional probability of failure Pr_{failure} of the component in the time interval $[t_S, t_{WF}]$, given that the component already has survived until t_S is:

$$Pr_{\text{failure}} = 1 - \frac{1 - CDF(t_{WF} | \mu, \sigma)}{1 - CDF(t_S | \mu, \sigma)} \quad (38)$$

where CDF is the cumulative lifetime distribution function with mean μ and standard deviation σ . The mean lifetime is calculated by equation (34) and the standard deviation according to section 4.4.

This model has been implemented in a stand alone Excel tool, and applied to the Lillgrund wind power plant as an example, estimating cost for both turbine transformers and the substation transformer. The model has been implemented for turbine transformers for illustration purposes only. In lack of model and design data for the materials in turbine transformers, data for cellulose-insulated transformers has been used. The data used is summarized in Table 6-2.

TABLE 6-2: DATA USED FOR THE TRANSFORMER EXAMPLE.

Parameter	Value	Comment/reference
Rated power (kVA)	120000	Lillgrund design documentation
DP_start	1000	Accepted value for cellulose-insulated transformers
DP_end	200	Accepted value for cellulose-insulated transformers
Activation energy, E_a (J/mol)	111000	[28]
Average for parameter A (/h)	1.6E+09	Assuming an average water content in the paper $w_{p,hs} = 2\%$
Universal gas constant R (J/mol/K)	8.31	-
Top oil temperature rise above ambient temperature at rated load (K)	51	Average value for some transformers in Norway investigated in Ref. [27]. Less conservative than example values from [29]
Average winding temperature rise above average oil temperature at rated load (K)	15	Average value for some transformers in Norway investigated in Ref. [27]. Less conservative than example values from Ref. [29]
Loss ratio	6	Example values from Ref. [29]
Oil exponent	0.8	Example values from Ref. [29]
Winding exponent	1.3	Example values from Ref. [29]
Std.deviation divided by mean for lifetime distribution	0.27	Based on limited statistics for some scrapped transformers in Norway investigated in Ref. [27]
Failure cost (EUR)	200 000 / 3 000 000	For turbine/substation, respectively. Example only. Must be supplied by the wind farm operator
Cooler type	KNAN / ONAN	For turbine/substation, respectively. Lillgrund design documentation
Ambient temperature	15 C	Constant temperature assumed for simplicity
Turbine power	Simulated 10 min average values for 35 hours	Simulated for Lillgrund by DTU. To be able to illustrate the model, these 35 hours are assumed representative for the whole transformer lifetime
Wind plant lifetime	20	Typical value

Power time series used cover a period of approx. 35 hrs and were simulated by DTU for the turbines in Lillgrund wind farm for both a baseline strategy without derating, and different derating strategies. For the simulations, a wind time series was used where the wind comes from a direction around 100° . The control strategy used in the transformer example presented below is 30% derating of the turbines in rows A and B; see Figure 6-9. For the transformer example and cost calculations, the turbines in column 3 were used, i.e. turbines that are affected by derating and wake effects.

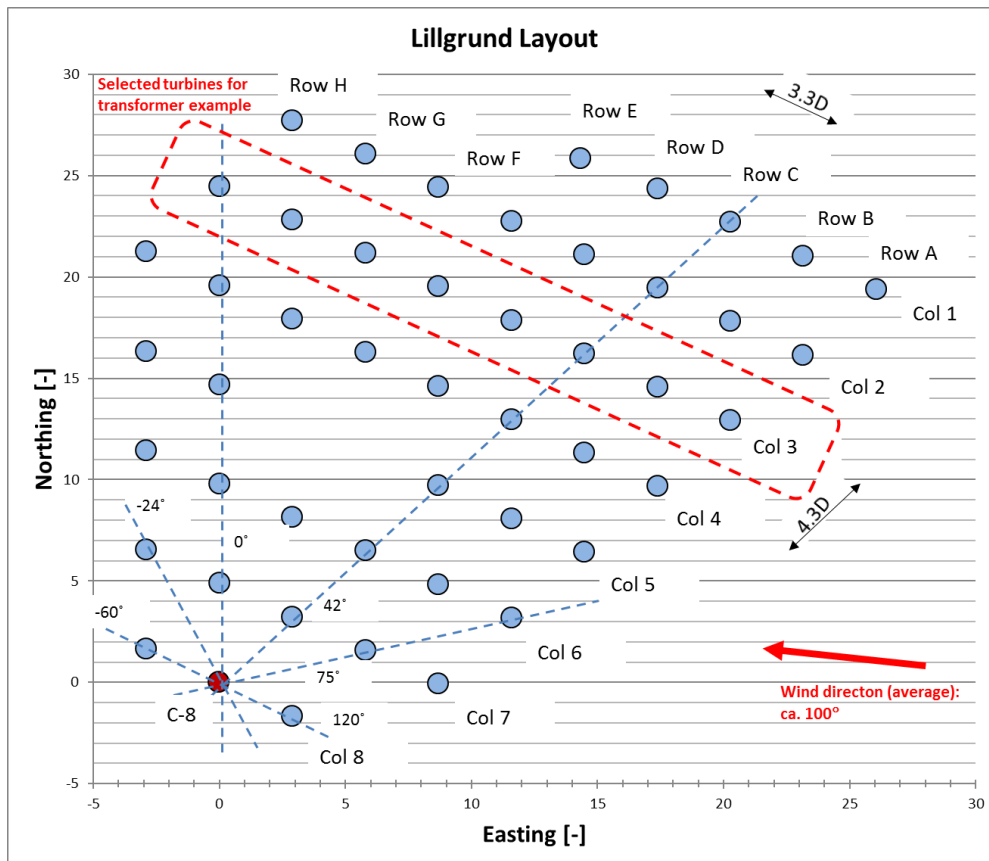


FIGURE 6-9: LILLGRUND WIND FARM LAYOUT AND SELECTED TURBINES FOR TRANSFORMER EXAMPLE.

Despite limited realistic data, the implementation illustrates well the use of the model. Selected results are given in the two figures below. Figure 6-10 shows the failure cost for selected turbine transformers for two control strategies, one without and one with derating. The wind direction is here such that the turbines C-H are in the wake from A-B, and therefore have somewhat lower power and hence lower failure cost in the case without derating. The results show that the derating has a large effect on the turbines in the A-B rows, but negligible effect on the other rows.

Figure 6-11 shows failure cost for the substation transformer for the same two control strategies, calculated by both the failure rate model and the lifetime distribution model. The results show that the failure rate model estimates a much larger failure cost. The large difference between the models is elaborated below.

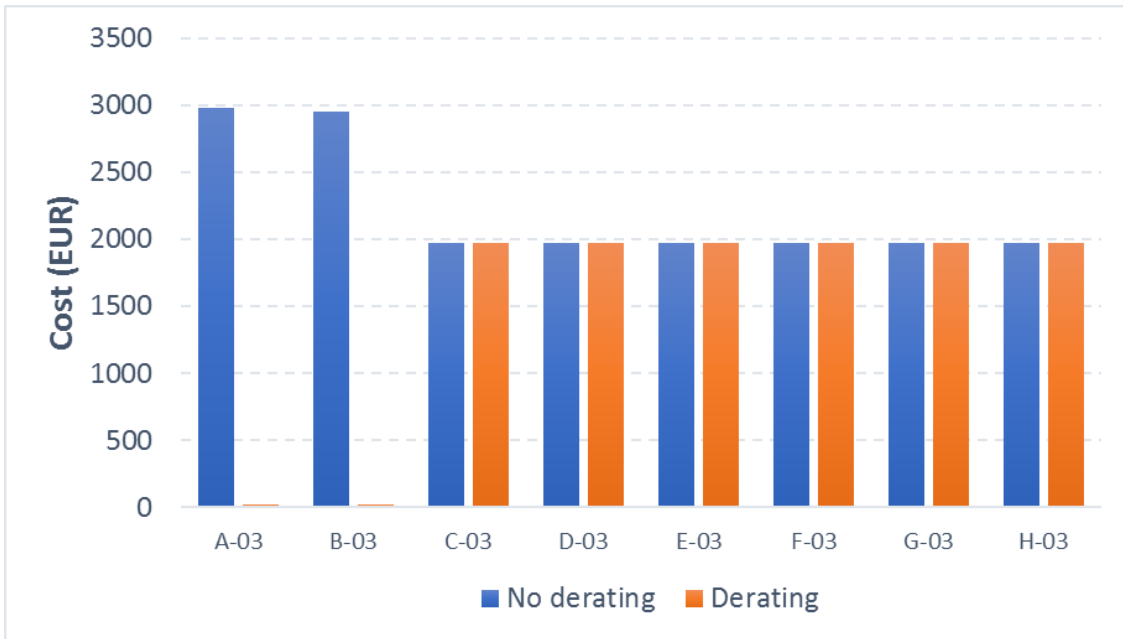


FIGURE 6-10: FAILURE COST FOR SELECTED TURBINE TRANSFORMERS FOR TWO CONTROL STRATEGIES, ONE WITHOUT AND ONE WITH DERATING. THE DERATING IS REDUCING THE POWER IN ROWS A AND B OF THE WIND FARM BY 30%

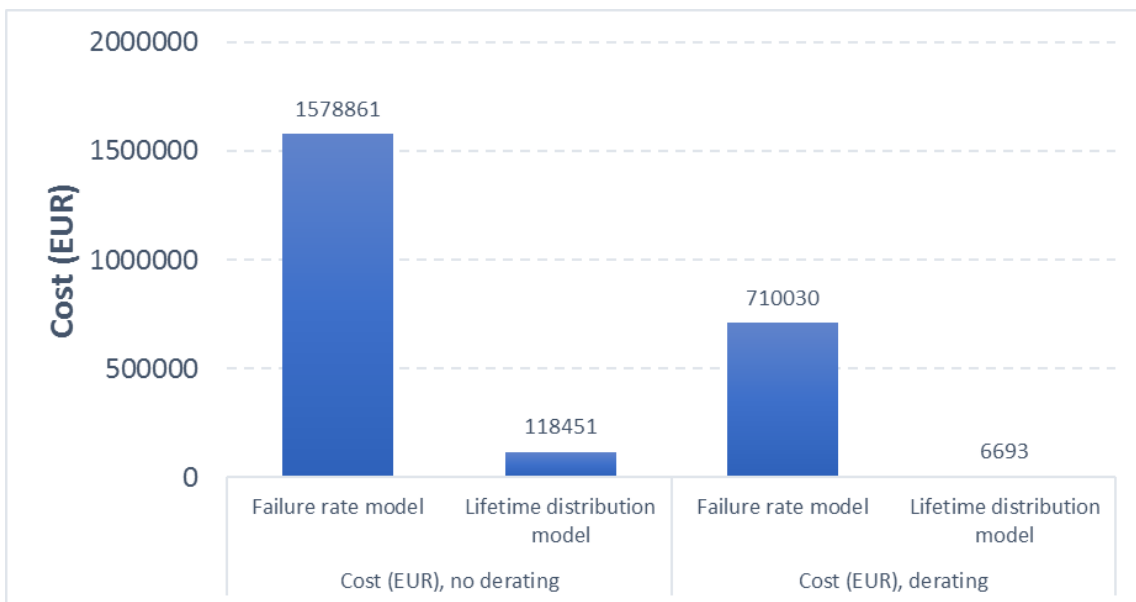


FIGURE 6-11: FAILURE COST FOR THE SUBSTATION TRANSFORMER FOR TWO CONTROL STRATEGIES, ONE WITHOUT AND ONE WITH DERATING, CALCULATED BY BOTH THE FAILURE RATE MODEL AND THE LIFETIME DISTRIBUTION MODEL. THE DERATING IS REDUCING THE POWER IN ROWS A AND B OF THE WIND FARM BY 30%

DISCUSSION

Aging of transformers is dominated by periods where the transformer is highly loaded combined with a high ambient temperature. Limiting such periods may be beneficial e.g. if the transformer is approaching its expected end-of-life, and it is desirable to keep the wind farm in operation longer. If, on the other hand, the estimated transformer lifetime is significantly longer than the design lifetime of the wind park, limiting the load is less relevant. In such cases, the

degradation cost of a control strategy will be small, as the transformer in any case is expected to outlive the wind park.

The reason for the difference between the failure rate model and the lifetime distribution model in the examples presented above is that the failure probability of the transformers is represented by the left tail of the lifetime distribution; see Figure 6-12. The failure probability within the wind farm lifetime is the accumulated probability of failure in the first 20 years. This is represented by the area below the probability density function (PDF), neglecting here the probability of more than one failure within the lifetime, which for the presented case is very low. For the failure rate model, the expected number of failures within the wind farm lifetime is represented by the area below the failure rate.

In Figure 6-12, both the failure rate for the failure rate model and the pdf for the Weibull distribution are plotted. Since the areas below the curves represent the failure probability or expected number of failures within the wind farm lifetime, as well as the corrective maintenance costs, we can see that the failure rate model heavily overestimates the costs when the component lifetime is significantly longer than the analysis period (here: the wind farm lifetime).

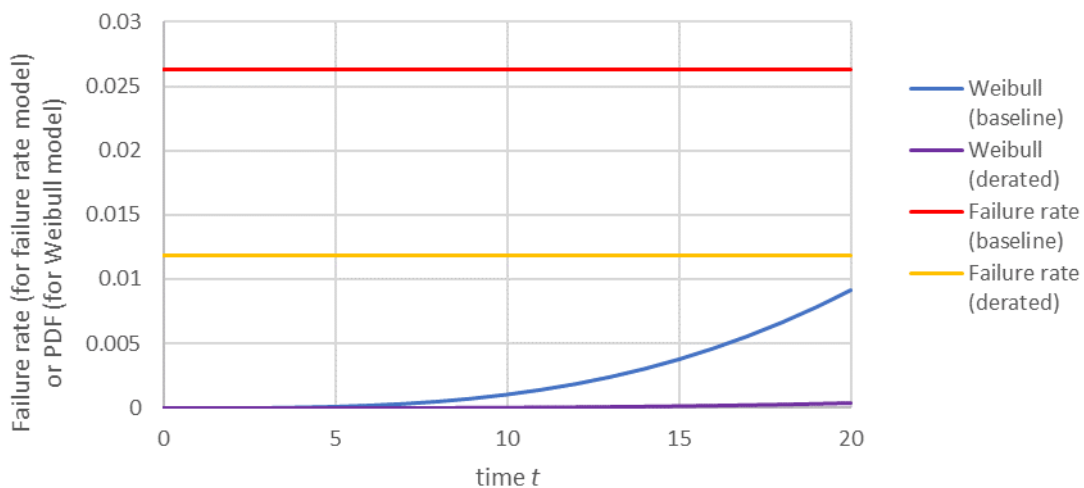


FIGURE 6-12: FAILURE RATE AND PDF FOR THE FAILURE RATE MODEL AND THE WEIBULL DISTRIBUTION MODEL, RESPECTIVELY.

The difference between the failure rate model and the lifetime distribution model depends not only on the relation between the component lifetime and the length of the analysis period, but also on the shape of the lifetime distribution. The shape of the distribution can be described by the coefficient of variation (CV). For the example presented above where the Weibull distribution was used, the shape can also be described by the Weibull shape parameter α . $CV=1$ and $\alpha=1$ mean that the Weibull distribution becomes an exponential distribution.

In Figure 6-13, the difference between the two cost models as function of the coefficient of variation and Weibull shape, respectively, is illustrated. The difference of the models is shown as ratio between the costs obtained by the failure rate model to the costs obtained by the Weibull distribution model, i.e. $C_{\text{Failure rate model}}/C_{\text{Weibull model}}$. If $C_{\text{Failure rate model}}/C_{\text{Weibull model}} = 1$, both models give the same result. Note that there is a small difference between the models, even though the Weibull distribution becomes an exponential distribution ($CV=1$ and $\alpha=1$), because the Weibull model ignores the cost contributions of the failures that

may happen within the analysis period after the first failure. However, if the component is non-repairable, the lifetime distribution model is without error, because the component can fail only once.

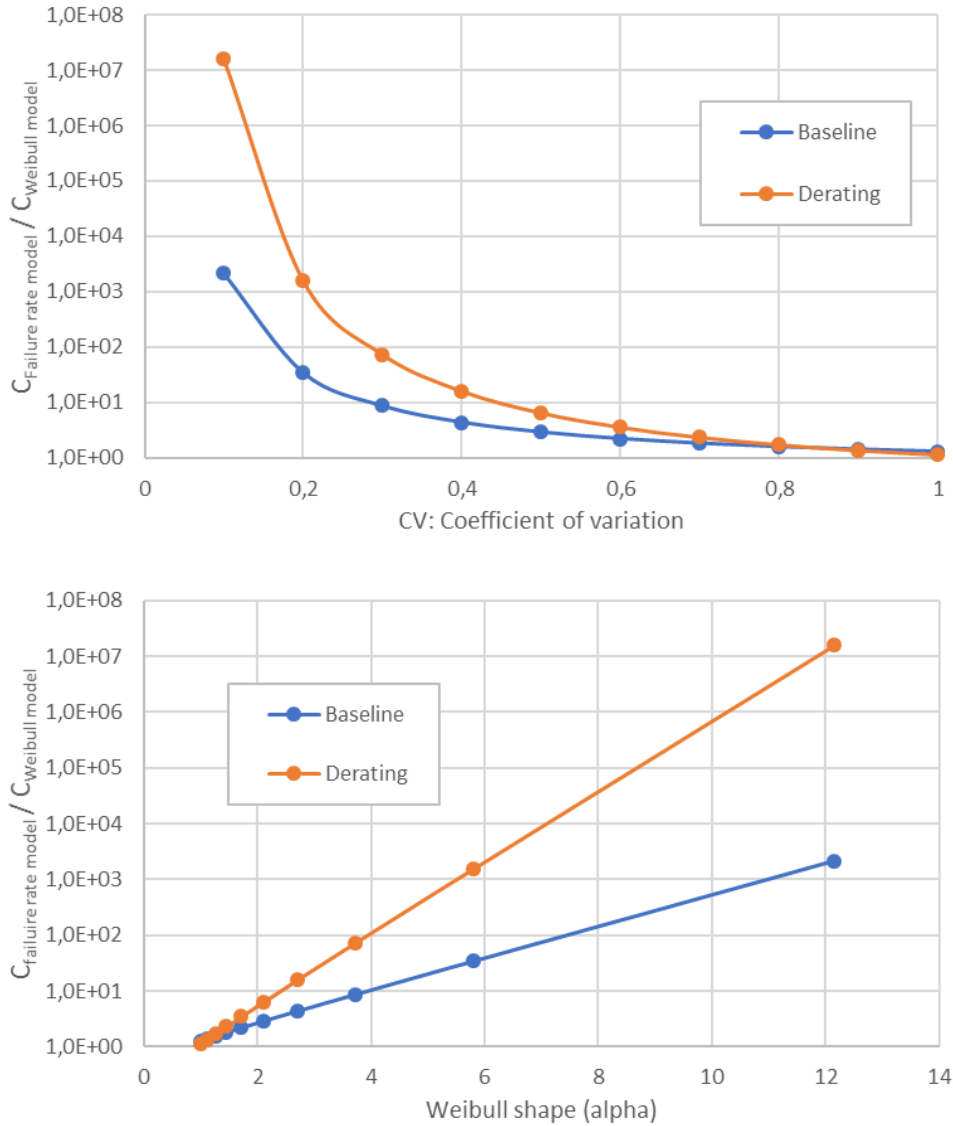


FIGURE 6-13: RATIO OF THE FAILURE RATE MODEL AND THE WEIBULL DISTRIBUTION MODEL AS FUNCTION OF THE COEFFICIENT OF VARIATION (TOP) AND THE WEIBULL SHAPE (BOTTOM).

The difference between the models can be reduced, when an adjusted failure rate is used; as also discussed in Appendix D. The adjusted failure rate is calculated as the failure rate that gives the same result as the Weibull model over the analysis period of 20 years wind farm lifetime. The adjusted failure rates are for both the baseline and derated case are shown in Figure 6-14.

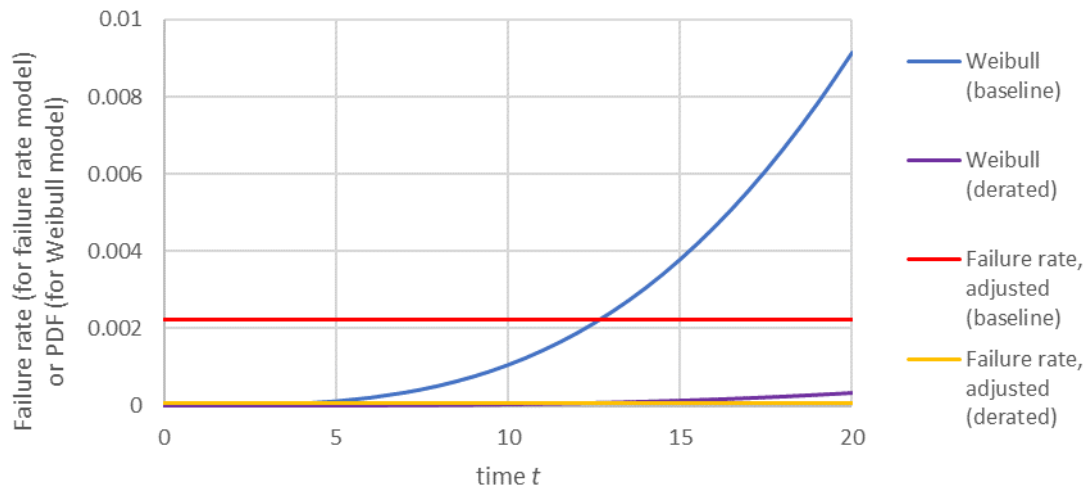


FIGURE 6-14: ADJUSTED FAILURE RATE AND PDF FOR THE FAILURE RATE MODEL AND THE WEIBULL DISTRIBUTION MODEL, RESPECTIVELY.

7. WIND FARM COST MODEL

The cost optimisation of a wind turbine is not in the scope of this work. Instead, the turbine design is assumed fixed, restricting the domain of optimisation to parameters that can be varied in real time. These are wind farm control parameters, such as yaw alignment and power set points.

Introducing yaw misalignment can steer the wake away from downwind turbines. Reducing the power set point can be done in two ways: via speed or torque. The aim for both of these is to reduce the energy deficit in the wake. This report does not model the effect of yaw because it requires high fidelity simulations. Instead, torque-based power derating is used.

7.1 DETAILS OF THE COST MODEL FRAMEWORK

The subsequent framework, based on the flowchart presented in Section 3.2, is presented in the following sub-sections: The first states and explains the desired outputs of the model. The second, third and fourth sections describe the calculations of the energy production, annual operating expenses and initial capital costs respectively. Finally, the fifth section will state the inputs required by the model to perform the aforementioned calculations.

OUTPUTS

The model shall return a series of statistics on energy production, Annual Operating Expenses, and Cost of Energy.

Energy production:

- AEP

Annual Operating Expenses:

- Cost of preventative and corrective maintenance
- Availability losses due to scheduled and unscheduled maintenance
- Utilisation of staff/equipment

Cost of Energy:

- Levelised Cost of Energy
- A breakdown of the sources of costs

INTERMEDIATE CALCULATIONS

Herein the non-trivial calculations of each component shall be described, starting from the outputs, working back towards the inputs.

The *energy production statistics* shall be calculated based upon a PDF of the power produced by the wind farm. This PDF shall be calculated from the *turbine performance* of each turbine in the farm (accounting for *wind farm effects* such as wake losses), the *availability* of each turbine and the PDF of the *metocean data* (parameterised as a Weibull distribution).

The *annual operating expenses* shall be calculated as the sum of the *service personnel & equipment costs* (assumed to be a fixed annual price) and the product of the cost and expected number of failures (may be non-integer) for each component.

The *downtime* shall be calculated as the sum of the time required for scheduled and unscheduled maintenance of each component. Each of these repair durations is multiplied by the inverse of the accessibility to account for the differing levels of access for each vehicle required for component maintenance.

The *accessibility* shall be calculated as the probability that each vehicle will be able operate according to its metocean limits.

The *unscheduled maintenance* and *scheduled maintenance* shall calculate the expected number of failures and replacements (both may be non-integer) and the repair time associated with each from the mean time between failure and service intervals along with the direct time to repair.

Component costs and the total *Initial Capital Costs* will either be provided manually as an input or estimated based on key turbine parameters such as rating and rotor diameter [31].

INPUTS

To perform the aforementioned calculations, certain parameter will need to be known, and provided to the model. The primary inputs are stated below but this list is not exhaustive:

- Metocean, in the form of Weibull distribution parameters
- Turbine performance data (power, speed, torque and thrust curves) of each turbine provided by BLADED/windfarmer including wake and electrical losses
- Component data including cost, MTBF and minimum and maximum service intervals
- Economic data on Producer Price Index (PPI) and exchanges rates
- Service personnel and equipment data

FACTORS NOT ACCOUNTED FOR

Some factors which will impact costs are not currently accounted for. These factors are either too computationally demanding, not well enough understood to be quantified, or minimally influential. These factors are listed below:

- Failures caused by exceeding of limit loads
- Influence of component age on MTBF
- Scheduling and allocation of maintenance
 - Availability of parts
 - Lead time on parts orders
 - Vehicle capacity – people and parts
 - Vehicle and staff availability
 - Time/resources required to diagnose failure before fixing it
 - Repair time may be non-continuous due to shift times and weather conditions
 - Reduce maintenance time by utilising spare technicians
 - Opportunistic maintenance – where preventative maintenance is completed alongside corrective maintenance to reduce number of deployments of resources
- *Accessibility* and *downtime* will differ between wind turbines and depend on wind speed

7.2 DETAILS OF INDIVIDUAL COMPONENT MODELS

This section of the report details the individual component models including the origin of the model, the terminology and the equations themselves. Each model can operate independently of the others, with the exception that outputs from one model may be inputs to another. The title of each subsection corresponds with its respective block of the flowchart. The cost model has been implemented in an excel sheet showing the cost evaluations and can be downloaded from

[https://share.dtu.dk/sites/TotalControl_140500/Deliverables/D2.1%20Cost%20model%20for%20fatigue%20degradation%20and%20O%20and%20M%20\(M12\)/Combined%20Wake-Fatigue%20Model.xlsm?Web=1](https://share.dtu.dk/sites/TotalControl_140500/Deliverables/D2.1%20Cost%20model%20for%20fatigue%20degradation%20and%20O%20and%20M%20(M12)/Combined%20Wake-Fatigue%20Model.xlsm?Web=1)

WAKE CALCULATIONS

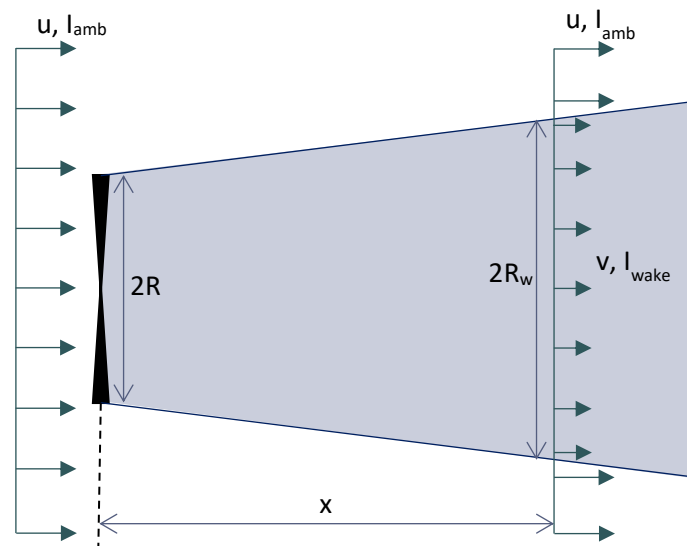


FIGURE 7-1: WAKE BEHIND A TURBINE ROTOR OF RADIUS R . WAKE RADIUS GROWS TO R_w AT DISTANCE x .

The following notation is used for the wake calculations presented below:

A_s	Area swept by the rotor [m ²]	u_∞	Freestream wind speed of the wind farm [m.s ⁻¹]
C_t	Thrust coefficient	v	Wind speed in the wake [m.s ⁻¹]
I_+	Additional turbulence	x	Distance aft of the turbine [m]
I_0	Ambient turbulence	x_n	Length of the near wake region [m]
I_{wake}	Total turbulence in wake	z_0	Roughness length [m]
r	Radial distance from centre of wake [m]	τ	Tip speed ratio
R	Blade radius [m]	ρ	Air density [kg.m ⁻³]
R_w	Radius of the wake [m]	Ω	Rotor speed [rad.s ⁻¹]
$R_{9.6}$	Radius of the wake 9.6 diameters downstream [m]	dr/dx	Wake growth rate
T	Thrust [N]	$(dr/dx)_m$	Growth rate due to shear-generated turbulence
u	Wind speed upstream of the turbine [m.s ⁻¹]	$(dr/dx)_\alpha$	Growth rate due to ambient turbulence
		$(dr/dx)_\tau$	Growth rate due to mechanical turbulence

TURBULENCE

Quarton and Ainslie [32] examined a number of different sets of wake turbulence measurements, both in wind tunnels using small wind turbine models or gauze simulators, and behind full-size turbines in the free stream. An empirical formula for added turbulence downstream from the turbine was found to give a good fit to the various measurements. An improvement to the expression was proposed by Hassan which shall be used here [33]. For the purposes of this model two additional terms have been appended to this equation. First is a mask to distribute the additional turbulence radially within the wake. This term is defined to provide an identical shape to that found in velocity deficit. The second term is a scaling factor to represent the decrease in additional turbulence due to the increasing width of the wake. Due to the addition of these terms an additional correction may be required; hence the original linear factor of 5.7 has been replaced with a parameter γ_t which can be altered as needed. Figure 7-1 illustrates many of the following variables.

$$I_{wake} = \sqrt{I_0^2 + \sum_{all\ turbines} I_+^2} \quad (39)$$

$$I_+ = \gamma_t C_t^{0.7} I_0^{0.68} \left(\frac{x}{x_n}\right)^{-0.96} \left(1 - \left(\frac{r}{R_w}\right)^{\frac{3}{2}}\right) \frac{R}{R_w}$$

$$x_n = \frac{nr_0}{\frac{dr}{dx}}$$

$$n = \frac{\sqrt{0.214 + 0.144m}(1 - \sqrt{0.134 + 0.124m})}{(1 - \sqrt{0.214 + 0.144m})\sqrt{0.134 + 0.124m}}$$

$$r_0 = R \sqrt{\frac{m+1}{2}}$$

$$\begin{aligned}
 m &= \frac{1}{\sqrt{1 - C_t}} \\
 C_t &= \frac{T}{\frac{1}{2}\rho u^2 A_s} \\
 \frac{dr}{dx} &= \sqrt{\left(\frac{dr}{dx}\right)_\alpha^2 + \left(\frac{dr}{dx}\right)_m^2 + \left(\frac{dr}{dx}\right)_\lambda^2} \\
 \left(\frac{dr}{dx}\right)_\alpha &= 2.5I_{amb} + 0.005 \\
 \left(\frac{dr}{dx}\right)_m &= \frac{(1 - m)\sqrt{1.49 + m}}{(1 + m)9.76} \\
 \left(\frac{dr}{dx}\right)_\tau &= 0.012B\tau \\
 \tau &= \frac{\Omega R}{u}
 \end{aligned}$$

VELOCITY LOSSES

Larsen and Réthoré [34] developed a fast, closed-form semi-analytical model to approximate wake deficit for use in multi-fidelity wind farm optimisation that preserves the essential physics of the problem.

The core of the model is a split of scales in the wake flow field, with large scales being responsible for stochastic wake meandering and small scales being responsible for wake attenuation and expansion in the meandering frame of reference as caused by turbulent mixing.

The problem is simplified by considering the wake as a perturbation on a mean flow. The apparent mean flow thus develops downstream in the wind farm both due to conventional shear (due to e.g. roughness changes) and due to wake contributions, which expand in space and therefore attenuate with increasing downstream distance from the wake emitting turbines.

Gradients of mean flow quantities being much bigger in the radial direction than in the axial along wind direction, leads to a wake model formulation based on the thin shear layer approximation of the Navier-Stokes equations. With this basis, further simplification is gained from a dimension reduction (from three to two) resulting from an assumption of rotational symmetry of the wake deficit. With the assumption of rotational symmetry follows in turn implicitly the need for a rotationally symmetric inflow field for the wake deficit prediction – in practice though a uniform inflow field.

Considering the approximate character of the proposed stationary wake deficit prediction, only the first order model is considered to be of practical importance.

Velocity behind individual turbine:

$$\Delta u = -\frac{u}{9} (C_t A_s (x + x_0))^{-2} \frac{1}{3} \left(r^{\frac{3}{2}} (3c_1^2 C_t A_s (x + x_0))^{-\frac{1}{2}} - \left(\frac{35}{2\pi} \right)^{\frac{3}{10}} (3c_1^2)^{-\frac{1}{5}} \right)^2 \quad (40)$$

$$x_0 = \frac{9.6(2R)}{\left(\frac{R_{9.6}}{kR}\right)^3 - 1}$$

$$c_1 = (kR)^{\frac{5}{2}} \left(\frac{105}{2\pi}\right)^{-\frac{1}{2}} (C_t A x_0)^{-\frac{5}{6}}$$

$$R_{9.6} = k_1 \exp(k_2 C_t^2 + k_3 C_t + k_4) (k_5 I_0 + 1) 2R$$

$$k_1 = 0.435, k_2 = 0.798, k_3 = -0.125, k_4 = 0.136, k_5 = 15.6$$

$$k = \sqrt{\frac{\frac{1}{\sqrt{1-C_t}} + 1}{2}}$$

The term Δu is a function of radial location. For influence on downstream turbines the speed at the hub shall be evaluated and assumed uniform across the affected rotor. Alternative strategies such as the mean are suggested but are unlikely to be influential and therefore not worth the 2D numerical integration.

Size of wake:

$$R_w = \left(\frac{105 c_1^2}{2\pi}\right)^{\frac{1}{5}} (C_t A_s (x + x_0))^{\frac{1}{3}} \tag{41}$$

For locations inside the wake of multiple turbines, as illustrated in Figure 7-2, it is assumed that the kinetic energy deficit of the mixed wake is equal to the sum of the energy deficits of the individual wakes [35].

For interacting wakes:

$$\left(\frac{v}{u_\infty}\right)^2 - 1 = \sum \left[\left(\frac{u_i + \Delta u_i}{u_\infty}\right)^2 - \left(\frac{u_i}{u_\infty}\right)^2 \right] \tag{42}$$

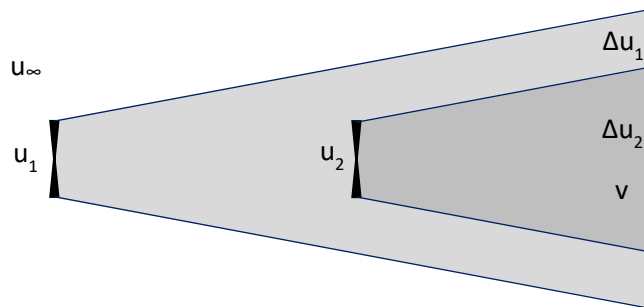


FIGURE 7-2: TWO TURBINES ARRANGED IN LINE WITH THE WIND DIRECTION. TURBINE 1 CREATES WIND SPEED DEFICIT Δu_1 AND TURBINE 2 CREATES ADDITIONAL WIND SPEED DEFICIT Δu_2 .

FATIGUE ACCUMULATION

The following notation is used for fatigue accumulation model:

B_c	Cost per failure [£/failure]	P_0	Power curve production [W]
B_d	Downtime per failure [£/failure]	P_d	Derated power production [W]
d	Derating	P_r	Rated power production [W]
D	Total damage	$Pr(u)$	Probability that wind speed u will occur
F_f	Relative flapwise fatigue of the blade	T_{dyn}	Normalised dynamic thrust
F_g	Relative fatigue of the gearbox	T_{st}	Static thrust [N]
F_p	Relative fatigue of the pitch system	u	Wind speed at the turbine [$m.s^{-1}$]
F_t	Relative fatigue of the tower and nacelle	u_{ci}	Cut-in wind speed of the turbine [$m.s^{-1}$]
I	Turbulence intensity	u_{co}	Cut-out wind speed of the turbine [$m.s^{-1}$]
I_d	Turbulence intensity designed for	u_{pci}	Cut-in wind speed of the pitch system [$m.s^{-1}$]
L_c	Cost losses [£]	α	Weibull shape parameter
L_d	Downtime losses [years]	β	Weibull scale parameter
m_b	Material coefficient for blades	$\theta(u)$	Steady state pitch at wind speed u [deg]
m_t	Material coefficient for towers	λ	Failure rate [failures/year]
N	Wind farm lifespan [years]	$\sigma()$	Standard deviation of ()

Equations for the fatigue of the main turbine components were formulated by DNV GL based on their experience in the field and historical data - explanations of the equations are stated below each one respectively. The units aren't representative of physical damage (for example damage equivalent load is used as a measure); therefore, the equations are used to calculate the changes in damage compared to a baseline case. Variations in the dynamic thrust cause variation in mechanical loading and thereby material strain. This is quantified using the dynamic thrust, which is raised to the material coefficient to give damage.

$$F_f = T_{dyn}^{m_b} \quad (43)$$

Gearboxes fatigue linearly with power. This is because each tooth experiences a local force proportional to the gearbox torque and experiences a number of cycles of that force that is proportional to the gearbox speed.

$$F_g = \frac{P_d}{P_r} \quad (44)$$

The tower fatigues proportional to the magnitude of the dynamic thrust, raised to the tower material coefficient.

$$F_t = T_{dyn}^{m_t} \quad (45)$$

The pitch systems fatigue due to accumulated pitch travel, which we approximate as proportional to the gradient of the pitch-speed curve at the current wind speed, multiplied by the current variation in wind speed. We normalise by the turbulence intensity the turbine was designed for.

$$F_p = u \frac{I}{I_d} \frac{d\theta}{du} \quad (46)$$

It should be noted that the pitch system will actuate the derating and therefore its operational conditions will be affected by this. It can be assumed that if derating is applied, the pitch angle

data will be translated to represent the pitch system cutting in at a new, lower, velocity. The new pitch cut in velocity is the velocity at which the derating first influences the power output of the turbine.

$$T_{dyn} = \frac{Iu}{I_d u_{co}} T_{st} \frac{P_d}{P_0} \quad (47)$$

The turbine is designed for loading proportional to $\sigma(u_d) = I_d u_{co}$. The turbine experiences $\sigma(u) = Iu$ and the ratio of these terms captures the increase in magnitude of fatigue cycles that will occur at high turbulence values. The static thrust term accounts for the damage amplification that occurs due to the static deformation of the blade. When the power production is reduced due to derating, some loads are reduced due to higher pitch angles than when operating on the nominal power curve. However, the pitch system will have an increase in fatigue, since it is being used to regulate the rotor speed over a wider wind speed range.

$$P_d = \min\{P_0, P_r(1 - d)\} \quad (48)$$

This comes from the definition of derating, where the power is limited to a fraction of the rated power of the turbine. The mean damage and power are calculated weighted by the probability of the respective wind speed occurring.

$$D_* = \int \text{Pr}(u) \times F_* du \quad \forall * \in \{f, g, t, p\} \quad (49)$$

We assume wind speeds follow a Weibull distribution, as is commonplace.

$$\text{Pr}(u) = \frac{\alpha}{\beta} \left(\frac{u}{\beta}\right)^{\alpha-1} e^{-\left(\frac{u}{\beta}\right)^\alpha} \quad (50)$$

CORRECTIVE MAINTENANCE

For modelling the influence of fatigue and damage reduction on costs, the failure rate model as described in section 4.4 is used. The failure rate for the case with derating can be calculated:

$$\lambda = \frac{D}{D_{baseline}} \lambda_{baseline} = \varepsilon \lambda_{baseline} \quad (51)$$

Where ε is the failure rate adjustment factor as introduced in section 4.4.

From this each failure mode can have its associated lifetime cost and downtime calculated. For consumable parts (parts that are replaced when they fail) the expected number of failures is calculated and subsequently used to calculate the repair cost and repair time:

$$\begin{aligned} L_c &= \lambda N B_c \\ L_d &= \lambda N B_d \end{aligned} \quad (52)$$

For non-consumable parts (parts not replaced at failure that result in a non-operational turbine) there is no repair cost, but the downtime is the expected remainder of the life of the turbine. Due to the low failure rate of these types of failure, the Poisson-based failure distribution is approximately constant which can be integrated to calculate the expected downtime losses:

$$L_c = 0 \quad (53)$$

$$L_d = \lambda \frac{N^2}{2}$$

8. CONCLUSIONS

This report has given a comprehensive introduction to failure models, which forms the foundation to component-specific failure and cost models for offshore wind farms. Where relevant, physical phenomena have been included in models, e.g. wake and thermal effects.

Models were presented that can be used to calculate O&M costs as a function of turbine operation and control. The intention is to use these models to reduce cost of energy in offshore wind farms with respect to wind farm control parameters.

Both electrical and mechanical components have been discussed. The application of the models is illustrated by several examples. Some of the models are also implemented in an Excel workbook, allowing turbine layout, costs, failure rates and control parameters to be defined. The equations in that model are implementations of those in this report.

Future work may focus on:

- Components that are not explicitly addressed in this report (e.g. generator)
- The use of Monte Carlo techniques to explore the impact of parameter uncertainty
- More detail on maintenance, e.g. scheduling inspections, weather impacts, etc.

REFERENCES

- [1] J. Carroll, A. McDonald and D. McMillan, "Failure rate, repair time and unscheduled O&M cost analysis of offshore wind turbines," *Wind Energy*, vol. 19, pp. 1107-1119, 2016.
- [2] O. Anaya-Lara, J. O. Tande, K. Uhlen and K. Merz, *Offshore wind energy technology*, Wiley, 2018.
- [3] W. Meeker and L. Escobar, *Statistical methods for reliability data*, John Wiley & Sons, 1998.
- [4] G. C. Larsen, H. Aagaard Madsen, N. Troldborg, T. J. Larsen, P.-E. Réthoré, P. Fuglsang, ... and P. Frohböse, "TOPFARM - next generation design tool for optimisation of wind farm topology and operation.," DTU, Risø National Laboratory for Sustainable Energy, Roskilde, 2011.
- [5] G. C. Larsen, "A simple generic wind farm cost model tailored for wind farm optimization," DTU, Risø National Laboratory for Sustainable Energy, Roskilde, 2009.
- [6] T. Bjørkvoll and B. Bakken, "Calculating the Start-Up Costs of Hydropower Generators," in *Proceedings IEEE 14th Power Systems Computational Conference (PSCC)*, Sevilla, 2002.
- [7] M. Rausand and A. Høyland, *System reliability theory: Models, statistical methods, and applications*, Hoboken: Wiley, 2004.
- [8] H. Ascher and H. Feingold, *Repairable systems reliability: modeling, inference, misconceptions and their causes*, New York: CRC Press/Marcel Dekker, 1984.
- [9] B. Bakken and T. Bjørkvoll, "Hydropower unit start-up costs," in *Proceeding IEEE Power Engineering Society Summer Meeting*, Chicago, 2002.
- [10] P. K. Chaviaropoulos and A. Natarajan, "A Simplistic Approach for Translating Load Reduction Potential to Cost Reduction," INNWIND.EU deliverable report D1.25, 2017.
- [11] A. Natarajan and T. Pedersen, "Remaining Life Assessment of Offshore Wind Turbines Subject to Curtailment," *Proceedings of the Twenty-eighth (2018) International Ocean and Polar Engineering Conference*, 2018.
- [12] B. Le and J. Andrews, "Modelling wind turbine degradation and maintenance," *Wind Energy Journal*, vol. 19, pp. 571-591, 2016.
- [13] S. D'Arco, T. Undeland, M. Bohlander and J. Lutz, "A Simplified Algorithm for Predicting Power Cycling Lifetime in Direct Drive Wind Power Systems," in *SSD 2012*, Chemnitz, 2012.
- [14] U. Scheuermann and S. R., "Investigation on the VCE(T)-Method to Determine the Junction Temperature by using the Chip Itself as Sensor," in *PCIM*, 2009.
- [15] T. Bryant, P. A. Mawby, P. R. Palmer, E. Santi and J. L. Hudgins, "Exploration of Power Device Reliability Using Compact Device Models and Fast Electrothermal Simulation," *IEEE Transactions on Industry Applications*, vol. 44, no. 3, pp. 894-903, Jun. 2008.
- [16] R. Bayerer, T. Herrmann, T. Licht, J. Lutz and M. Feller, "Model for Power Cycling lifetime of IGBT Modules - various factors influencing lifetime," in *5th International Conference on Integrated Power Systems (CIPS)*, 2008.
- [17] Vattenfall Vindkraft AB, "Technical description Lillgrund wind power plant," 2008.
- [18] DuPont Nomex 410 technical data sheet:
http://www.dupont.com/content/dam/assets/products-and-services/electronic-electrical-materials/assets/DPT16_21668_Nomex_410_Tech_Data_Sheet_me03_REFERENCE.pdf

- .
- [19] IEEE 1276-1997, "IEEE guide for the application of high-temperature insulation materials in liquid-immersed power transformers," 1997.
 - [20] Empire State Electric Energy Research Corporation, "Improved emergency rated power transformers," report EP86-24, 1987.
 - [21] W. J. McNutt et al., "Thermal life evaluation of high temperature insulation systems and hybrid insulation systems in mineral oil," *IEEE trans. power del.*, 1996.
 - [22] International Electrotechnical Commission, "Power transformers - Part 14: Liquid-immersed power transformers using high-temperature insulation materials," *IEC 60076-14*, 2013.
 - [23] M. Wen et al., "Reliability assessment of insulation system for dry type transformers," *IEEE*, 2013.
 - [24] J. Song et al., "The aging characteristics of the Nomex paper for the flameproof dry-type transformer," *IEEE*, 2016.
 - [25] C. Ranga et al., "Life assessment of TUK and Nomex 910 impregnated mineral transformer oils using Raman spectroscopy," in *CATCON*, 2017.
 - [26] S. Shuhang, "Comparative investigation on the properties of transformer-used high-temperature resistand oil and paper insulation materials," thesis, 2016.
 - [27] SINTEF Energy Research, "Trafotiltak - Analyse av behov for diagnose, vedlikehold eller utskifting av krafttransformatorer," report, 2018.
 - [28] L. Lundgaard et al., "Transformer windings - ageing, diagnosis and asset management," *SINTEF Energy Research TR A7099*, 2015.
 - [29] International electrotechnical commission, "Power transformers - Part 7: Loading guide for oil-immersed power transformers," *IEC 60076-7*, 2005.
 - [30] International Electrotechnical Commission, "Mineral insulating oils in electrical equipment - supervision and maintenance guidance," *IEC 60422*, 2013.
 - [31] L. Fingersh, M. Hand and A. Laxson, "Wind Turbine Design Cost and Scaling Model," NREL, 2006.
 - [32] D. C. Quarton and J. F. Ainslie, "Turbulence in wind turbine wakes," *Wind Engineering*, vol. 14, no. 1, pp. 15-23, 1990.
 - [33] U. Hassan, "A wind tunnel investigation of the wake structure within small wind turbine farms," Energy Technology Support Unit, Harwell Laboratory, 1993.
 - [34] G. C. Larsen and P. E. Réthoré, "A simple stationary semi-analytical wake model," Risø National Laboratory for Sustainable Energy, Technical University of Denmark, Roskilde, Denmark, 2009.
 - [35] I. Katic, J. Højstrup and N. O. Jensen, "A simple model for cluster efficiency," in *European wind energy association conference and exhibition*, 1987.
 - [36] M. I. Blanco, "The economics of wind energy," *Renewable and sustainable energy reviews*, vol. 13, no. 6-7, pp. 1372-1382, 2009.
 - [37] A. Myhr, C. Bjerkseter, A. Ågotnes and T. A. Nygaard, "Levelised cost of energy for offshore floating wind turbines in a life cycle perspective," *Renewable Energy*, vol. 66, pp. 714-728, 2014.
 - [38] W. Short, D. J. Packey and T. Holt, "A Manual for the Economic Evaluation of Energy Efficiency and Renewable Energy Technologies," National Renewable Energy Laboratory,

Golden, Colorado, 1995.

- [39] B. Snyder and M. J. Kaiser, "Ecological and economic cost-benefit analysis of offshore wind energy," *Renewable Energy*, vol. 34, pp. 1567-1578, 2009.
- [40] C. Bjerkseter and A. Ågotnes, "Levelised costs of energy for offshore floating wind turbine concepts," Norwegian University of Life Sciences, 2013.
- [41] I. Dinwoodie¹, O.-E. V. Endrerud, M. Hofmann, R. Martin and I. B. Sperstad, "Reference cases for verification of operation and maintenance simulation models for offshore wind farms," *Wind Energy*, vol. 39, no. 1, pp. 1-14, 2015.
- [42] T. Burton, N. Jenkins, D. Sharpe and E. Bossanyi, *Wind energy handbook*, John Wiley & Sons, 2011.
- [43] R. Barthelmie, G. Larsen, S. Frandsen, L. Folkerts, K. Rados, S. Pryor, B. Lange and G. Schepers, "Comparison of wake model simulations with offshore wind turbine wake profiles measured by sodar," *Journal of atmospheric and oceanic technology*, vol. 23, no. 7, pp. 888-901, 2006.
- [44] G. Osburn, "Hydrogenerator Start / Stop Costs," U.S. Department of the Interior, Bureau of Reclamation, Technical Service Center, 2014.
- [45] [Online]. Available: <http://www.dupont.com/products-and-services/personal-protective-equipment/thermal-protective/brands/nomex/products/nomex-papers.html>.

APPENDIX A – LITERATURE REVIEW

The economics of wind energy [36]

This article presented the outcomes of a study carried out among wind energy manufacturers and developers regarding the current generation costs of wind energy projects in Europe, the factors that most influence them, as well as the reasons behind their recent increase and their expected future evolution.

The main learning points are summarised below:

- The key parameters that govern wind power costs are:
 - Initial capital costs (wind turbines, foundations, road construction and grid connection) which can be as much as 80% of the total cost of the project over its lifetime.
 - O&M costs can constitute up to 30% of overall costs for offshore wind farms.
 - The electricity produced (dependant on wind climate and wind turbine technical specifications).
 - The discount rate and economic lifetime of the investment.
- The cost of fuel and O&M are much lower than conventional methods. In a natural gas power plant, for example, as much as 40–60% of the costs are related to fuel and O&M.
- The regulation defining who bears the connection cost and the upgrade of the grid differs in each country.
- Construction and installation techniques for offshore projects are less developed than for onshore projects, impacting both cost and reliability.
- Offshore O&M costs are substantially higher than for onshore projects, largely due to the higher cost of transport and reduced site access.

Wind Turbine Design Cost and Scaling Model [31]

This report detailed the National Renewable Energy Laboratory's work to develop a reliable tool for estimating the cost of wind-generated electricity, for both onshore and offshore wind turbines.

The main learning points are summarised below:

- Economic indicators such as the Gross Domestic Product (GDP) and Producer Price Index (PPI) may be necessary to account for the changes in price of materials, parts and labour with time.
- Cost estimates of turbine components can be made based upon turbine rating, rotor diameter, hub height, and other key turbine descriptors either directly or by using these to estimate mass and assuming a cost per unit weight.
- Levelised Cost of Energy (LCoE) has been used by DoE for some years to evaluate the total system impact of any change in design. It is calculated using a simplified formula that attempts to limit the impact of financial factors so that the true impact of technical changes can be assessed.

Levelised cost of energy for offshore floating wind turbines in a life cycle perspective [37]

This report presented a comprehensive analysis and comparison of the LCoE for the following offshore floating wind turbine foundation concepts: Spar-Buoy (Hywind II), Tension-Leg-Spar

(SWAY), Semi-Submersible (WindFloat), Tension-Leg-Wind-Turbine (TLWT) and Tension-Leg-Buoy (TLB).

The main learning points are summarised below:

- Depth is the dominant parameter to determine the optimal foundation type for a site. Distance to shore, Load Factor and availability are amongst the significant factors affecting the LCoE.
- At around 30 m, the monopile design reaches engineering limits with respect to pliable diameters and wall thicknesses. For deeper waters, the more expensive jacket foundation is a valid option. It is limited to depths of less than 50 m, not due to engineering limitations, but economic viability.
- Energy from floating wind turbines, in comparison to bottom-fixed concepts, may be produced at equal or lower LCoE. As more shallow wind farm sites become occupied, deep water foundations improve and LCoE become increasingly competitive, expect increasing amounts of floating deep water wind farms.
- The focus for floating foundation designers should be to reduce the demand for line axial stiffness in order to compete in deeper waters. This may be one means by which control can be influential (potentially by controlling thrust) in future.

A Manual for the Economic Evaluation of Energy Efficiency and Renewable Energy Technologies [38]

This report provides guidance on economic evaluation approaches, metrics, and levels of detail required, while offering a consistent basis on which analysts can perform analyses using standard assumptions and bases.

The main learning points are summarised below:

- Costs that are normally included in O&M are frequently recurring labour and materials costs required to keep a system in operation. They can be broken into the following categories: those costs that occur only when the system is operating (variable O&M costs) and those fixed costs that do not vary with the output of the system but rather are required to keep the system in an operable state.
- Infrequent (once or twice during the analysis period) major repair and replacement usually should be considered separately from O&M. The more common method of accounting for these significant repairs and replacements is to assume that the repair or replacement occurs at the end of the component's expected useful life, discount the repair or replacement cost to its present value at the beginning of the analysis period, then add it to the initial investment cost.
- For mature technologies, O&M cost estimation is generally based on historical performance. However, for renewable energy systems that are typically in the early stages of technical and market development, O&M costs are more difficult to estimate.

Ecological and economic cost-benefit analysis of offshore wind energy [39]

This report discusses the costs and benefits of offshore wind relative to onshore wind power and conventional electricity production.

The main learning points are summarised below:

- To compare renewables and conventional electricity production methods, the costs of market based carbon offsets should be included.

- The costs of offshore wind are a factor of 2–3 more expensive than either onshore or conventional electricity.
- The distance to shore influences both the construction and operation and maintenance costs, transport vessel hire and fuel costs and increased amounts of transfer cables to lay and maintain.

Failure rate, repair time and unscheduled O&M cost analysis of offshore wind turbines [1]

This report provides a detailed, quantitative breakdown of the failures modes, frequencies, costs, repair times for offshore wind turbines.

The main learning points are summarised below:

- The reliability of an offshore wind turbine and the resources required to maintain it can make up to 30% of the overall cost of energy.
- Due of accessibility, the importance of reliability increases as offshore wind energy generation increases.
- The biggest contributor to the overall failure rate for offshore wind turbines is the pitch and hydraulic systems.
- Each component can have multiple failure modes, of differing severity.
- Failure rate varies from year to year. Turbine sub-systems with higher failure rates (such as the pitch and hydraulic system) do not follow the bathtub curve. However, some turbine components, such as the converter and electrical components show more of a resemblance to a bathtub curve.
- Failure rates increase with wind speed. Impact is more significant for offshore compared to onshore.
- There is no observable correlation between turbulence intensity and failure rates.
- There is an inverse relationship between downtime for each failure mode and number of technicians deployed to a failure.
- Failure rates are higher for offshore turbines than onshore turbines. Due to:
 - Higher wind speeds
 - Worse maintenance standard due to comparatively low access
 - Larger turbine (known to have higher failure rates)
 - Harsh environment (reaches sealed components during maintenance)
- Contains useful data which may be needed in cost model

Levelised Costs of Energy for Offshore Floating Wind Turbine Concepts [40]

The main purpose of the thesis is to evaluate and compare Life Cycle Costs and Levelised Costs of Energy for a series of fictitious wind farms consisting of wind turbines of different conceptual or realised designs, located far offshore.

The main learning points are summarised below:

- The so-called bathtub curve is widely used in reliability engineering
- The offshore wind industry is not yet mature enough to provide accurate data as to how component-specific bathtub data are expected to vary.
- Maintenance can be subdivided into preventive and corrective
- Opportunistic maintenance (where unplanned corrective maintenance is combined with preventive maintenance carried out on other components) can reduce mobilisation and transport time and costs of vessels

- The most cost effective maintenance strategy balances maintenance costs and the cost of loss of production
- Specific components may fail in various modes
- Annual underwater inspections are required
- Schedule maintenance during summer when wind speeds are lower and accessibility is higher
- Must also consider failure of inter-array and export cables
- Can base maintenance team offshore
- It may be profitable to buy own vessels for both installation and O&M purposes, feasible for farms in excess of 100 units
- Instead of deploying large vessel to site it is possible to tow floating wind turbines to shore.

Reference Cases for Verification of Operation and Maintenance Simulation Models for Offshore Wind Farms [41]

This paper provides an approach for verifying O&M simulation models. A reference offshore wind farm is defined and simulated using these models to provide test cases and benchmark results for verification for wind farm availability and O&M costs.

The main learning points are summarised below:

- Due to the novelty of offshore wind energy generation and lack of real data, full validation is not possible.
- Annual direct O&M costs comprise of vessel, technician and repair costs.
- Discrete event, time-sequential Monte Carlo simulation using constant failure rates experiments appears to be the standard method for O&M models.
- Major replacements needing heavy lift vessels (HLVs) accounts for the majority of direct O&M costs but only make a moderate impact on availability.
- Some models allowed maintenance tasks to be completed in one deployment or failures to occur whilst turbine is inoperative.

Wind Energy Handbook [42]

This text book provides all major aspects of wind turbine design and operation citing basic external models where applicable such as:

- An empirical formula for added turbulence downstream from a turbine created by Quarton and Ainslie. The formula is based on a number of different sets of wake turbulence measurements, both in wind tunnels using small wind turbine models or gauze simulators, and behind full-size turbines in the free stream. The formula was found to give a good fit to the various measurements.

Comparison of Wake Model Simulations with Offshore Wind Turbine Wake Profiles Measured by Sodar [43]

This paper gives an evaluation of most of the commonly used models for predicting wind speed decrease (wake) downstream of a wind turbine as of 2005.

The main learning points are summarised below:

- For turbine spacing of between 4 and 8 rotor diameters, power losses due to wind turbine wakes can be expected to be in the range 5%–15% of the power output from the whole wind farm.
- Spacing beyond 8–10 D is unlikely due to the high cost of installing undersea cables to the wind farm.
- Average ambient turbulence offshore is typically between 6% and 8% at heights of about 50 m, compared with 10%–12% over land. The low turbulence intensity at offshore locations leads to a slower wake recovery and therefore to a longer near wake.
- Offshore turbulence has a minimum at 10–12m.s⁻¹ and then increases due to higher roughness at greater wind speeds.
- Ambient turbulence may be less relevant in large wind farms where turbulence generated by the wind turbines themselves is likely to dominate.

A simple model for cluster efficiency [35]

This paper details a simplified linear model for wake size and velocity deficit propagation to be used in a computationally efficient evaluation of the power capture of a wind farm.

The main learning points are summarised below:

- Interacting wakes can be modelled by assuming the kinetic energy deficit of the mixed wake is equal to the sum of the deficits of each wake calculate at the downstream location.
- Accumulation of wake deficit will typically reach an equilibrium after 3-4 turbines/rows.

A simple stationary semi-analytical wake model [34]

This paper presents a closed-form semi-analytical model of the velocity deficit in wind turbine wakes. The model is designed to reduce computational requirements but retain the physics required to be relevant to the more complex, Dynamic Wake Model; therefore, wake meandering is accounted for.

The main learning points are summarised below:

- Gradients of mean flow quantities are much larger in the radial direction than in the axial. Therefore, an assumption of rotational symmetry can be employed to reduce the wake model from three-, to two-, dimensional.
- Expansion of stationary wake fields are believed to be significantly affected by meandering of comparable “narrow” free shear wake deficit fields as described by the Dynamic Wake Model. This effect can be approximately accounted for by imposing suitable empirical downstream boundary conditions on the wake expansion that depend on the rotor thrust and the ambient turbulence conditions, respectively.

APPENDIX B – OPERATING TIME

In this appendix, we discuss the concept of operating time. Furthermore, we introduce the concept of degradation-equivalent operating time as a measure of degradation. The concepts of operating time and degradation-equivalent operating time are not used in the examples presented in this report. However, the concepts have been used for modelling operating conditions of hydropower plants; see references in this appendix. Thus, the concepts might be of interest for future work and we therefore briefly describe them in this appendix.

The following notation is used in this appendix:

γ	Proportion of calendar time a component is in operation and degrading	t^W	Degradation-equivalent time
t	Calendar time	Δt	Time interval
t'	Operation time	$\Delta t'$	Time interval in operating time
		w	Degradation rate
		W	Accumulated degradation

Note that the operating time for some wind turbine components may be different from the operating time of the wind turbine itself, since not all components are operated when the wind turbine is operating and producing energy.

If the component is permanently in operation, the calendar lifetime of this component is the same as the operating lifetime. However, if the component is not in use in some periods, the calendar lifetime is "longer" than the operating lifetime.

If γ is the proportion of calendar time the component is in operation, the relation between calendar time t and operating time t' is

$$t' = \gamma \cdot t \quad (54)$$

where the notation ' indicates operating time.

An estimate of γ can be the portion of time in the year when the component is in operation, given that the operating condition in this year is representative for other years. $\gamma < 1$ means that when the operating time of a component can be extended by $\Delta t'$ (e.g. by load reduction as a consequence of derating), the lifetime of the component measured in calendar time will be extended by

$$\Delta t = \frac{\Delta t'}{\gamma} \quad (55)$$

which is "longer" than $\Delta t'$. The following example illustrates this:

We assume that one hour baseline ("normal") operation reduces the operational lifetime by one hour. In addition, we assume that a component is operated 1000 hrs each year and that there is a linear relationship between load, degradation and time. When during these 1000 hrs the load and wear is reduced by 50%, the load reduction during these 1000 hrs of operation will result in a lifetime extension (in operating time) of 500 hrs with normal operation, and a lifetime extension (in calendar time) of $\frac{1}{2}$ year, because 500 hrs normal operation time corresponds to $\frac{1}{2}$ year of calendar time in normal operation.

When the load during these 1000 hrs is increased by 100% (doubling) due to a special operating strategy, the lifetime in operational time will be reduced by 2000 hrs with normal operation, and the lifetime (in calendar time) will be reduced by two years; one year given by the actual calendar time that is passed during the one year where the 1000 hrs are operated, and a second (additional) year by additional degradation as a consequence of loads above the normal situation that correspond to additional 1000 hrs of normal operation. Thus, the additional lifetime reduction for this special operating strategy is one year.

B.1 DEGRADATION-EQUIVALENT OPERATING TIME AS DEGRADATION MEASURE

A *degradation-equivalent operating time* t^w can be defined as an alternative measure of degradation in cases where it is difficult to define a physical measure of degradation, such as crack length, DP-value, etc. This concept was used by Bakken and Bjørkvoll [9] [6] to model the start-stop costs of hydropower units. The assumption is that a component is designed for specific number of hours of degradation-equivalent operating time, and that different operational and control events and different operating states consume different numbers of hours of degradation-equivalent operating time, e.g. that 1 hr of normal operation (i.e. hydropower turbine operates at best efficiency point, BEP) consumes 1 hr degradation-equivalent operating time and 1 start-stop cycle consumes 10 hrs of degradation-equivalent operating time [44]. This means that one start-stop is equivalent with 10 hrs normal operation regarding consumption of operating time t^w .

The concept of degradation-equivalent operating time is not further used in the work presented in this report. In the previously cited hydropower examples [9] [6], the degradation-equivalent operating time is used to quantify the effect of the operational events "start-up" and "shut-down" on the lifetime. The advantage is that the concept is easy to communicate. It has therefore been applied together with expert judgement [44], where experienced plant personnel or other persons with in-depth component knowledge judged the effects of unfavourable operating events and states, compared with optimal operating conditions. That is, experts were asked how much lifetime are consumed in the unfavourable operating conditions (e.g. start and stop) compared to normal operating conditions (e.g. operation at BEP). The concept of degradation-equivalent operating time has been applied to hydropower generators. In this report, a degradation and O&M cost model has not been presented for wind turbine generators. Further research work may focus on if the models for hydropower generators can be transferred to wind power applications.

B.2 RELATION BETWEEN DEGRADATION, OPERATING TIME AND CALENDAR TIME

The basic relation between degradation, operating time and calendar time is illustrated in the figure below (see also [9] and [6] for further discussions). In Figure B-1, we assume that γ , the proportion of calendar time the component is in operation, is 1. We also assume that there is a constant degradation rate $w = \Delta W / \Delta t$ that is constant over the whole lifetime. In this case, $t' = t$, i.e. operating time is equal to calendar time.

In Figure B-2, we have periods where the component is not in operation. We assume that the component does not degrade in these periods. Furthermore, we assume that we have a period where the degradation rates are reduced or increased due to operation in operational states with reduced or increased loads. In the second example, $t' < t$.

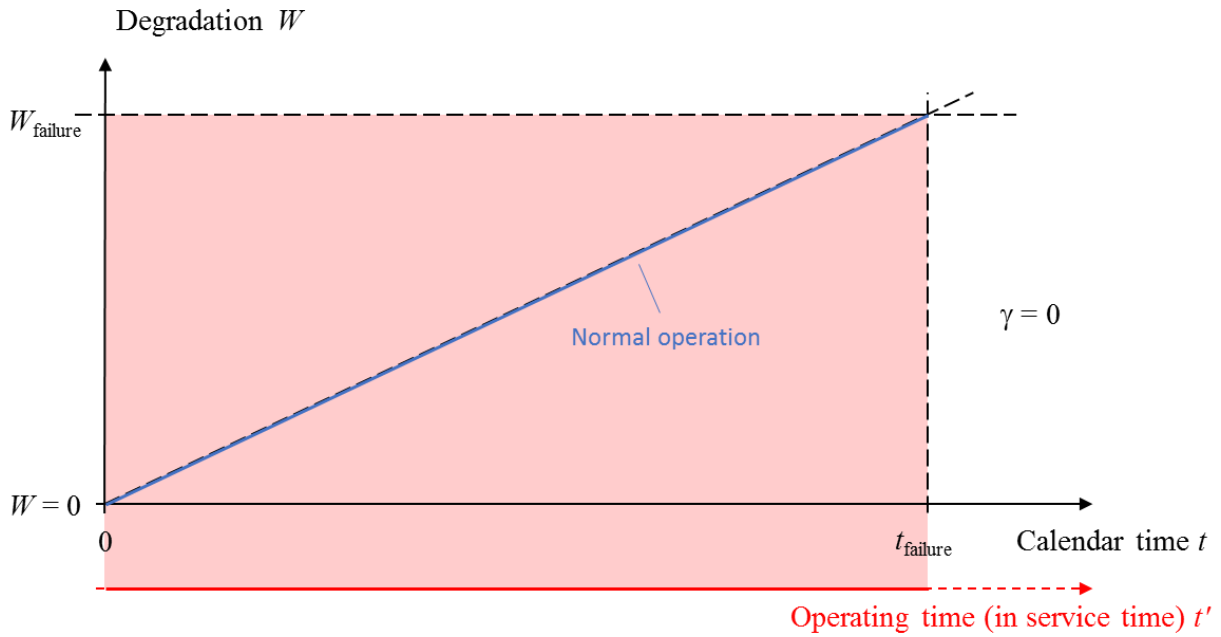


FIGURE B-1: RELTION BETWEEN CALENDAR TIME, OPERATING TIME AND DEGRADATION - CONTINUOUS OPERATION.

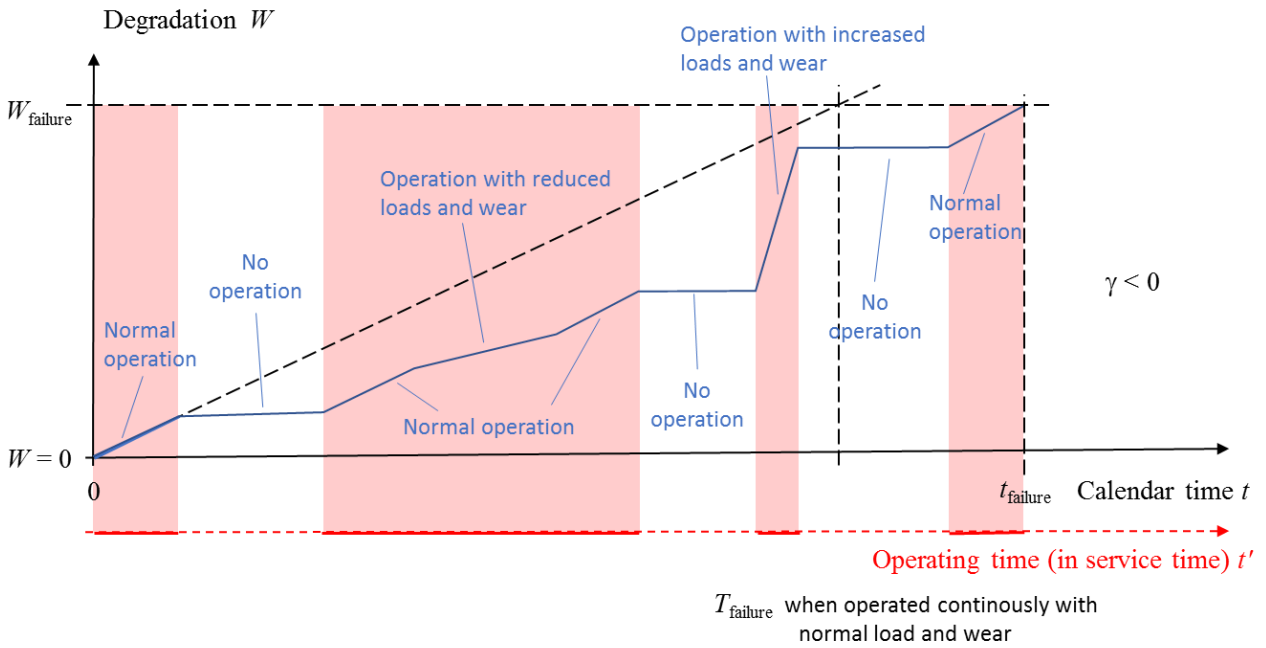


FIGURE B-2: RELATION BETWEEN CALENDAR TIME, OPERATION TIME AND DEGRADATION - DIFFERENT OPERATING STATES.

APPENDIX C – FAILURE RATE MODEL AND RELATION TO DEGRADATION

In this appendix, we justify the basic failure rate adjustment model by a very simple example where lifetime/failure rate are related to degradation. Then, we extend the simple example to a situation where the new control strategy is not applied to the whole lifetime, as in the basic model, but to shorter time periods that may represent periods with different control strategies.

The following notation is used in this appendix:

ε	Failure rate adjustment factor	w	Degradation rate
λ	Failure rate	W	Accumulated degradation
$MTBF$	Mean time between failure		
Δt_{CS}	Time interval with special control strategy		

C.1 RELATION BETWEEN LIFETIME/FAILURE RATE AND DEGRADATION

We assume that a wind turbine component accumulates over time degradation, as discussed and illustrated in section 4.1. The degradation per time interval, i.e. the degradation rate, is denoted w . We assume linear degradation, i.e. w is constant.

The accumulated degradation $W_{\text{baseline}} = MTBF_{\text{baseline}} \cdot w_{\text{baseline}}$ for the baseline control strategy is expected to result in failure of the component after the time interval $MTBF_{\text{baseline}}$. When reducing the degradation rate from w_{baseline} to w_{CS} , the time $MTBF_{CS}$ is assumed to be where accumulated degradation is the same for both the baseline strategy and the new strategy (see Figure C-1):

$$W_{\text{baseline}} = MTBF_{CS} \cdot w_{CS} = W_{CS} \quad (56)$$

Assuming that the degradation rate with special control actions is reduced with the factor ε from w_r to w_{CA} we get

$$w_{CS} = \varepsilon \cdot w_{\text{baseline}} \quad (57)$$

and

$$W_{\text{baseline}} = MTBF_{\text{baseline}} \cdot w_{\text{baseline}} = MTBF_{CS} \cdot \varepsilon \cdot w_{\text{baseline}} = W_{CS} \quad (58)$$

$$MTBF_{CS} = \frac{MTBF_{\text{baseline}}}{\varepsilon}$$

Since the mean time between failure $MTBF$ is the inverse of the failure rate λ , we have:

$$\lambda_{CS} = \frac{1}{MTBF_{CS}} = \frac{\varepsilon}{MTBF_{\text{baseline}}} = \lambda_{\text{baseline}} \cdot \varepsilon \quad (59)$$

This means that we can use the relative change of the degradation rate to adjust the failure rate. This is only valid for situations where the control actions are applied over the whole wind

farm lifetime, and when there is a (in average) constant degradation rate and a linear relation between degradation and lifetime.

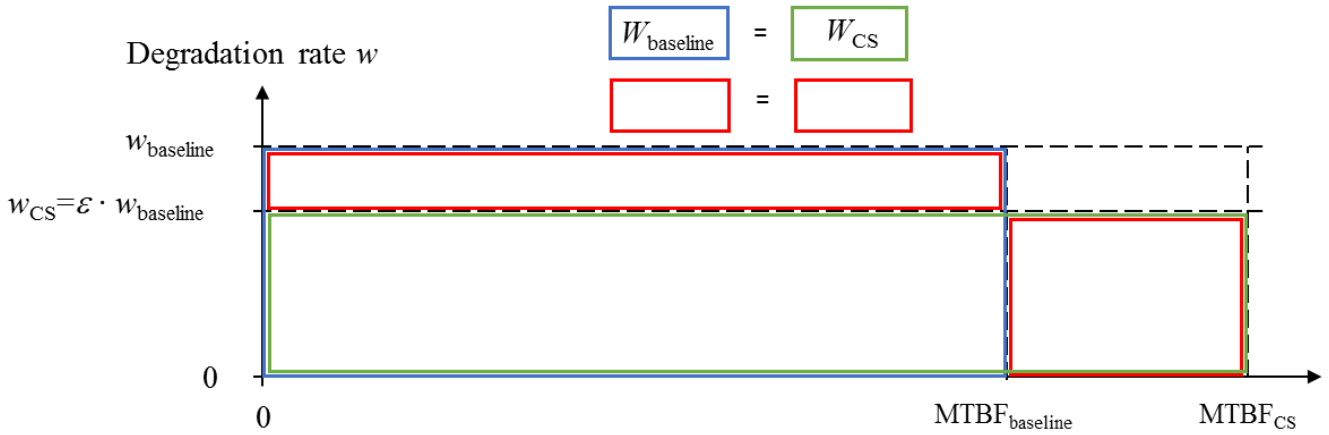


FIGURE C-1: REALTION BETWEEN DEGRADATION RATE AND MTBF FOR DIFFERENT CONTROL STRATEGIES.

C.2 EXTENSION TO CASES WHERE CONTROL STRATEGY IS APPLIED TO SHORTER PERIODS

In the following, the model is extended to situations where the control strategy is applied to a shorter time interval Δt . In Figure C-2, the situation for reducing the degradation rate from w_{baseline} to $w_{\text{CS}} = \varepsilon \cdot w_{\text{baseline}}$ in the time interval Δt_{CS} is illustrated. Note that Δt_{CS} is measured in calendar time, and not operating time (see Appendix B for a discussion of operating time and calendar time), when $MTBF$ is also given in calendar time. The reduction of degradation increases the lifetime and the mean time between failure from $MTBF_{\text{baseline}}$ to $MTBF_{\text{CS}}$. The lifetime extension is $\Delta MTBF = MTBF_{\text{CS}} - MTBF_{\text{baseline}}$. We assume that that the "degradation saving" (red area in the figure) is utilized after $MTBF_{\text{baseline}}$ with a control strategy that corresponds to the baseline strategy, i.e.:

$$\Delta MTBF \cdot w_{\text{baseline}} = (w_{\text{baseline}} - \varepsilon w_{\text{baseline}}) \cdot \Delta t_{\text{CS}} \quad (60)$$

$$\Delta MTBF = (1 - \varepsilon) \cdot \Delta t_{\text{CS}}$$

and

$$MTBF_{\text{CS}} = MTBF_{\text{baseline}} + \Delta MTBF = MTBF_{\text{baseline}} + (1 - \varepsilon) \cdot \Delta t_{\text{CS}} \quad (61)$$

Thus, the failure rate is:

$$\lambda_{\text{CS}} = \frac{1}{MTBF_{\text{CS}}} = \frac{1}{\frac{1}{\lambda_{\text{baseline}}} + (1 - \varepsilon) \cdot \Delta t_{\text{CS}}} \quad (62)$$

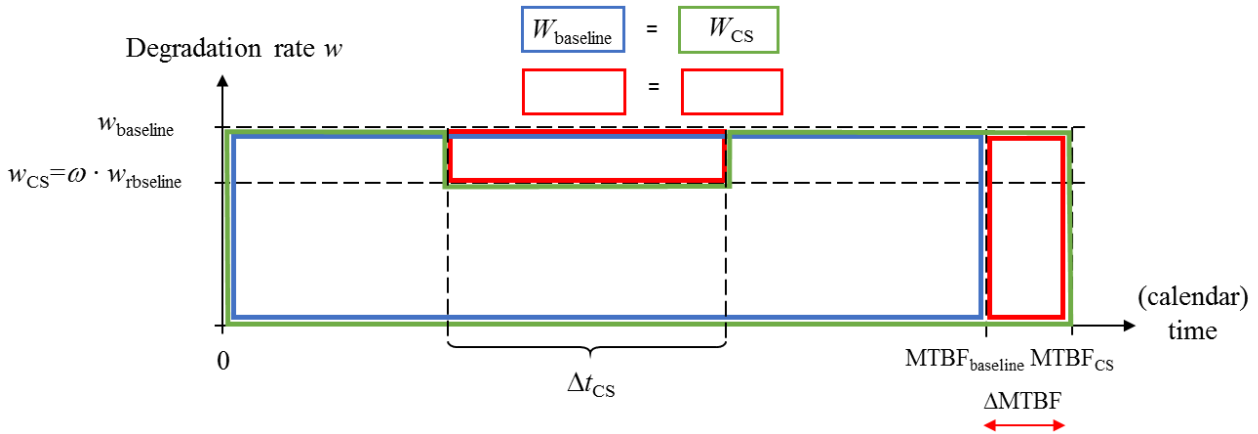


FIGURE C-2: REALTION BETWEEN DEGRADATION RATE AND MBF FOR DIFFERENT CONTROL STRATEGIES.

The model where the load is reduced by $(1 - \varepsilon)\%$ in the time interval Δt_{CS} is additive, because we can add the lifetime extension of $\Delta MTBF$ to $MTBF_{baseline}$ to receive $MTBF_{CS}$. $MTBF_{CS}$ can then be used as new baseline lifetime, which again can be extended by a new period with load reduction. The same is valid for the failure rate, where the load reduction in Δt_{CS} results in a new failure rate λ_{CS} . λ_{CS} is then the new baseline failure rate, which can be further reduced in a second period of load reduction (and so on).

APPENDIX D – FAILURE RATE AND HAZARD RATE

In this appendix, we briefly discuss the differences and similarities between failure rate (rate of occurrence of failure – ROCOF) and hazard rate (force of mortality – FOM) and how they influence the models presented in this report, the model results and the potential application of the models. The differences and similarities of failure rate (ROCOF) and hazard rate (FOM) were already briefly discussed in Section 4.4. This appendix extends the discussions and may provide more information and understanding, especially to the reader who is not so familiar with the topic. We refer to [8] where a thorough discussion of the concepts of FOM and ROCOF is given.

Figure D-1 shows the failure rate (blue line) for a component that is put into operation at $t = 0$ and replaced or repaired to a condition as good as new after failure. Note that the blue curve shown in the figure is the ROCOF and not the FOM. The lifetime (time to failure) of the component is modelled by a Weibull distribution with mean time to failure μ and shape parameter $\alpha = 4$. In the figure below, the time axis is normalized with μ .

When collecting failure data for such a component, or a population of such components, over a very long time, we would find out that the average failure rate (ROCOF) is as shown by the red horizontal line in the diagram. The probability density function (PDF) and the hazard rate of the Weibull distribution are also illustrated in the figure (green colour).

The first failure can be predicted with the Weibull distribution. The first failure will probably occur around 1μ , illustrated by the first maximum of the curve at 1μ . When coming to the prediction of the second and all following failures, we can see that the ROCOF with underlying Weibull model converges to a steady state situation. After approximately 4μ to 5μ , the Weibull model will develop to a constant failure rate of $1/\mu$, which is the same as the ROCOF of the constant failure rate model (assuming that repair times are neglectable). The reason for this development is that the uncertainty for prediction of failures very long ahead in time is quite high, i.e. from today's point of view, where we only know that the component is new at $t = 0$, the far future is more uncertain (and random) than the near future.

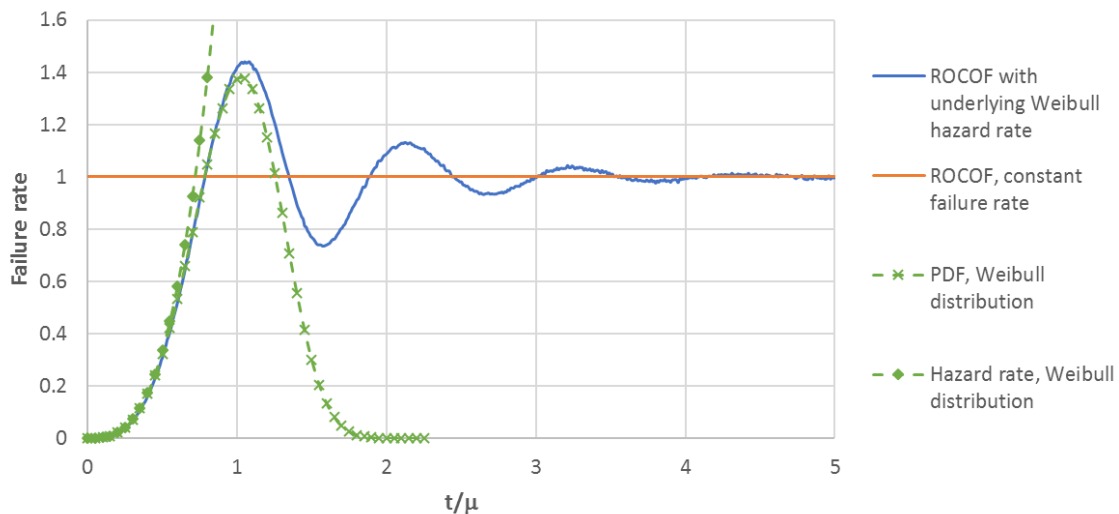


FIGURE D-1: FAILURE RATE – ROCOF WITH UNDERLYING WEIBULL HAZARD RATE, CONSTANT FAILURE RATE MODEL AND WEIBULL DISTRIBUTION (PDF AND HAZARD RATE).

When the analysis period (which could be the wind farm lifetime) is shorter than the component lifetime, the ROCOF with underlying Weibull hazard rate is best represented by the PDF of the Weibull distribution; see Figure D-2. The analysis period is highlighted in the figure, and we are interested in the yellow shaded area below the ROCOF with underlying Weibull hazard rate. This area is the expected (accumulated) number of failures in the analysis period. In this case, the lifetime distribution model (Weibull distribution) gives the best results.

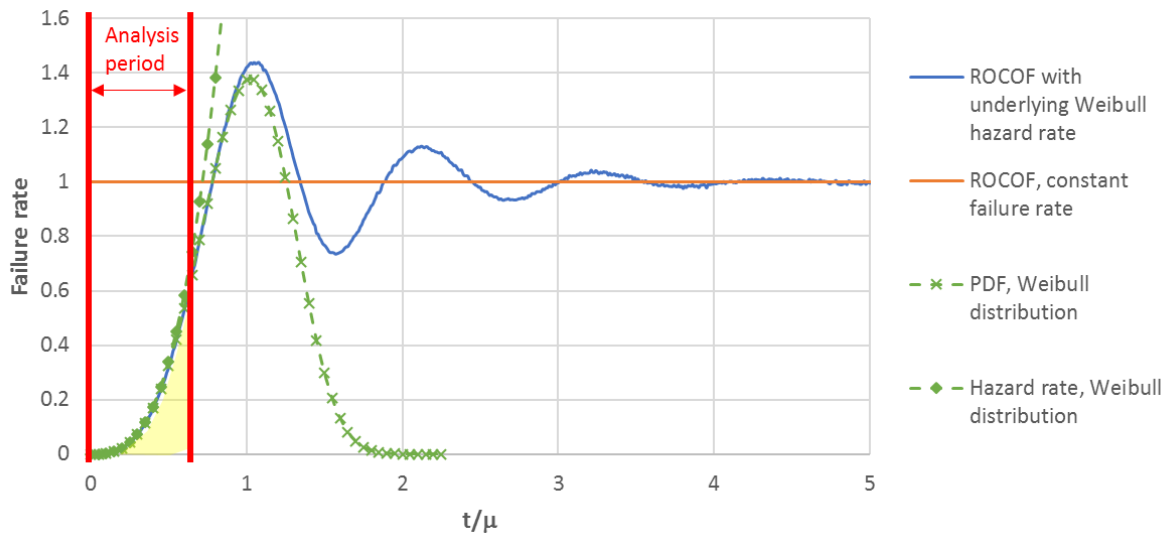


FIGURE D-2: CASE WHERE ANALYSIS PERIOD IS SHORTER THAN COMPONENT LIFETIME.

Instead of using the constant failure rate that represents a long-term average over a large number of life-cycles, one could use an adjusted failure rate as shown in Figure D-3 where the area below the failure rate is the same as the yellow area. When failure data is available from the analysis period, the failure rate calculated from this data is probably in the order of magnitude of the adjusted failure rate, since it only represent early failures. Then, both the failure rate model and the Weibull distribution model would give similar results.

If the analysis period is much longer than the component lifetime, illustrated by a larger red frame in Figure D-4. The failure rate model is the better model, because it represents the area below the ROCOF with Weibull hazard rate much better than the Weibull PDF.

Obviously, the best approach would be to calculate the ROFOF with underlying Weibull hazard rate. However, as already mentioned in Section 4.4, we usually need numerical methods for the calculation.

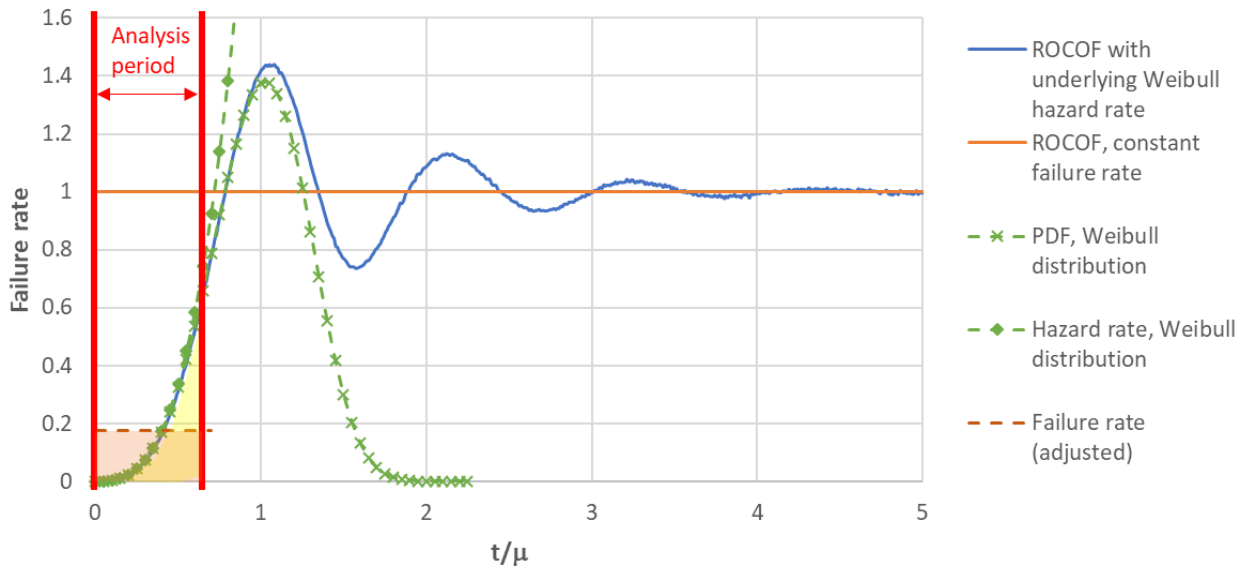


FIGURE D-3: CASE WITH SHORT ANALYSIS PERIOD AND ADJUSTED FAILURE RATE.

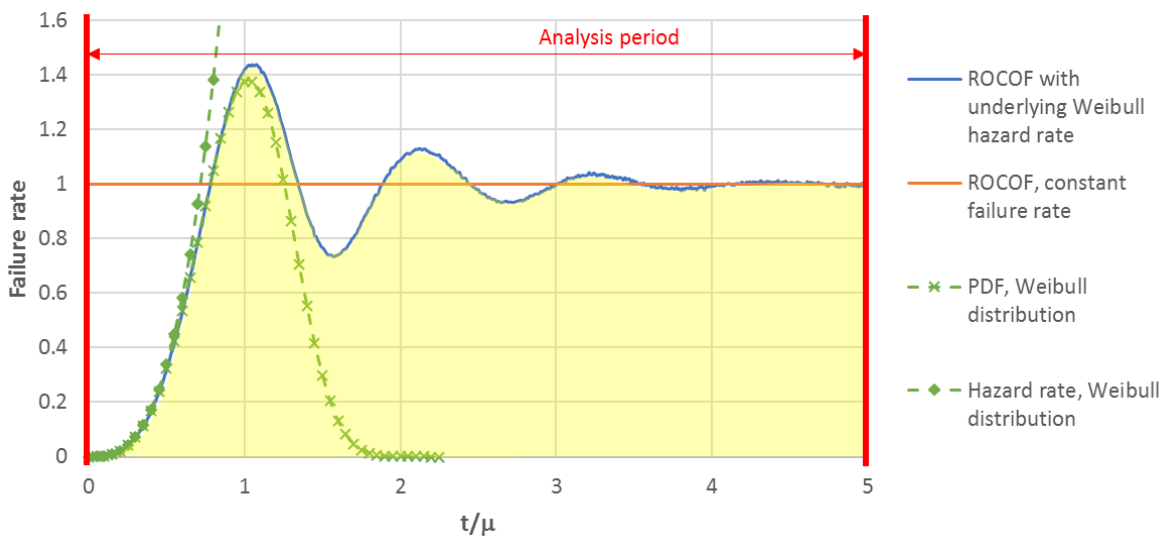


FIGURE D-4: CASE WHERE ANALYSIS PERIOD IS MUCH LONGER THAN COMPONENT LIFETIME.